

# A review of mass and energy flow through a lava flow system: insights provided from a non-equilibrium perspective

Simone Tarquini<sup>1</sup> 

Received: 22 July 2016 / Accepted: 8 July 2017 / Published online: 27 July 2017  
© Springer-Verlag GmbH Germany 2017

**Abstract** A simple formula relates lava discharge rate to the heat radiated per unit time from the surface of active lava flows (the “thermal proxy”). Although widely used, the physical basis of this proxy is still debated. In the present contribution, lava flows are approached as open, dissipative systems that, under favorable conditions, can attain a non-equilibrium stationary state. In this system framework, the onset, growth, and demise of lava flow units can be explained as a self-organization phenomenon characterized by a given temporal frequency defined by the average life span of active lava flow units. Here, I review empirical, physical, and experimental models designed to understand and link the flow of mass and energy through a lava flow system, as well as measurements and observations that support a “real-world” view. I set up two systems: *active lava flow system* (or ALFS) for flowing, fluid lava and a *lava deposit system* for solidified, cooling lava. The review highlights surprising similarities between lava flows and electric currents, which typically work under stationary conditions. An electric current propagates almost instantaneously through an existing circuit, following the Kirchhoff law (a least dissipation principle). Flowing lavas, in contrast, build up a slow-motion “lava circuit” over days, weeks, or months by following a gravity-driven path down the steepest slopes. Attainment of a steady-state condition is hampered (and the classic thermal proxy does not hold) if the supply stops before completion of the “lava circuit.” Although gravity determines initial flow path and extension,

the least dissipation principle means that subsequent evolution of mature portions of the active lava flow system is controlled by increasingly insulated conditions.

**Keywords** Mass and energy flow · Lava flow · Thermal proxy

## Introduction

The flanks of active basaltic volcanoes are often densely populated so that lava flows constitute a significant threat to property and infrastructure (e.g., Duncan et al. 1981; Mattox et al. 1993; Barberi et al. 2003; Rowland et al. 2005; Favalli et al. 2009, 2012a; Bartolini et al. 2014; Harris et al. 2016; Richter et al. 2016). However, the complexity of the thermal, rheological, and dynamic properties of a basaltic mixture of fluid, crystals, and vesicles has hampered a complete and unequivocal understanding of their emplacement, and a comprehensive connection between observations and theory is still missing. The problem that this issue raises is illustrated by the debate regarding derivation of lava discharge rate from the thermal signature of active lava flows (Dragoni and Tallarico 2009; Harris and Baloga 2009; Garel et al. 2015).

Efforts to determine a relation between the heat radiated from erupted lavas and the relevant mass dates back to the pioneering works of Yokoyama (1957) and Herdervari (1963), which quantified the amount of energy released by lavas emitted during selected eruptions, once the whole (known) volume of lava completely cooled down from eruption to ambient temperature. Later, Friedman and Williams (1968) used satellite infrared data for the first attempt to convert radiated energy to volume flux during the 1966 Surtsey eruption (Iceland).

Scandone (1979) included the heat carried by the volatile phase, and a comprehensive and vibrant account of the

---

Editorial responsibility: A. Harris

✉ Simone Tarquini  
simone.tarquini@ingv.it

<sup>1</sup> Istituto Nazionale di Geofisica e Vulcanologia - Sezione di Pisa, Pisa, Italy

progress in this field can be found in Harris (2013). For the purpose of the present work, one must mention the landmark work of Pieri and Baloga (1986), which proposed a linear relationship between discharge rate and lava plan area for Hawaiian lava flows. The so-called thermal proxy for the retrieval of the time-averaged discharge rate from the instantaneous heat loss at actively flowing lava is largely credited to those authors, who built upon earlier theoretical works (e.g., Danes 1972; Park and Iversen 1984). Further refinements of the original method of Pieri and Baloga (1986) have been provided by Crisp and Baloga (1990), Harris et al. (1997), Wright et al. (2001), and Harris et al. (2007a).

The *thermal proxy* is currently widely applied and provides generally consistent results (e.g., Harris and Ripepe 2007; Coppola et al. 2009; Vicari et al. 2009; Ganci et al. 2013). Harris and coworkers illustrated that the linear relationship between discharge rate and lava plan area is essentially empirical and needs to be scaled on a case-to-case basis to account for local conditions (e.g., rheological and topographic influences on flow spreading, Harris and Baloga 2009, Harris et al. 2010, Harris 2013). The linear relationship is also based on critical assumptions in the model (e.g., a constant flow thickness in the lava channel or a constant temperature of the crust), which are known to be a crude approximation of reality (Wright et al. 2001; Harris and Baloga 2009).

One of the controversial points of the classic *thermal proxy* approach is that a time-independent thermal steady state is assumed to apply. The existence of an initial transient time necessary to attain stationary conditions has been suggested by several authors (e.g., Garel et al. 2012, 2014, 2015; Coppola et al. 2013). Expanding on the theory of the *thermal proxy* (e.g., Wright et al. 2001), Coppola et al. (2013) introduced a “characteristic time” necessary for a spreading of the system to attain its maximum extent, but did not clarify how the characteristic time was linked to attainment of a thermal steady state. Instead, Garel et al. (2012, 2014, 2015) formulated their own thermal proxy (a *dynamic proxy*, as opposed to the classic or *static proxy*) through application of fluid dynamics theory coupled with analog experiments using both isoviscous and solidifying liquids. The point made by Garel et al. (2012, 2014, 2015) was that consideration of the fluid dynamics of cooling gravity currents permits a better understanding of the behavior of lava flows, allowing the transient time necessary to attain a thermal steady state to be assessed. However, the main issue of the *thermal proxy* is perhaps that, in spite of its considerable success, the basis of the method is empirical, and a clear physical foundation remains elusive (Dragoni and Tallarico 2009; Harris and Baloga 2009; Garel et al. 2012).

In reviewing the progress of the thermal approach over the years, it seems that a substantial effort has been produced in the development of methods for processing of the thermal signal, such as approaches to un-mix thermally mixed pixels (e.g., the dual band method of Dozier 1980 and following

refinements of Oppenheimer 1993; Flynn and Mouginitis-Mark 1994, McCabe et al. 2008). Somewhat less attention has, however, been paid in the interpretation of this signal in light of what we have learned in the meantime about the dynamics of lava flows. The impression is that there is a bridge to be constructed between different areas of knowledge in order to derive a more inclusive picture, and the present review is an attempt to move a step forward towards this goal.

In order to limit possible inconsistencies, I set out the present analysis starting from specific test cases which have been studied in detail, so that we can reasonably say that we know the “ground truth” of the lava dynamics (Hon et al. 1994; Self et al. 1998; Favalli et al. 2010; Tarquini and de’ Michieli Vitturi 2014 and references therein). The emitted thermal signal, being a consequence of the dynamics of the system, is considered later. Avoiding any critical assumptions about the thermal structure or the geometry of the lava body (e.g., a constant thickness of the flow, or a constant temperature of the crust), I identify a specific reference system which is taken to represent the main source of the thermal anomaly during lava emplacement. We will see that this is an open system (i.e., a system exchanging both mass and energy with its surroundings) that evolves consistently away from its thermodynamic equilibrium and which is arranged in structures constituted by lava flow units, a well-known entity (Nichols 1936; Walker 1971; Wadge 1978; Kilburn and Lopes 1988, 1991). Within the framework of non-equilibrium thermodynamics, this system can attain a non-equilibrium, but steady, state when the point of maximum heat dissipation is being approached. This point occurs when the mass of the system also approaches its maximum so that the rate of mass released from the open system equals the mass input. Review of mass and energy fluxes through the system clarifies the physical basis of the *thermal proxy* and also provides an explanation for the amount of time necessary to attain stationary conditions.

This theoretical understanding is then supported by a review of observed emplacement dynamics for different types of flow unit. While inflating sheet flows tend to approach a steady-state condition in a smooth and regular way, channelized flows are much more unstable, with high rates of heat and mass dissipation per unit length and frequent abandonment of old units followed by the birth of new ones that cause system instability. Finally, this review reveals unsuspected analogies between the basic energy balance equation for an active lava and the energy balance equations for an electric current or a gravity current (under steady-state conditions).

### **Lava flow emplacement: an open system evolving far from its thermodynamic equilibrium**

While magma remains stored underground below a volcano, the magmatic system exchanges very little energy and mass

with its surroundings and can be considered an adiabatic system that is evolving near the thermodynamic equilibrium (e.g., Mastin and Ghiorso 2001). When an effusive eruption occurs, the system experiences a transition from adiabatic conditions to strongly dissipative conditions (i.e., non-equilibrium) as the magma moves through the conduit (La Spina et al. 2016) and is emplaced on the Earth's surface. In the subaerial or submarine environment, lavas attain thermal equilibrium with their surroundings by releasing a large amount of heat (a temperature drop of order  $10^3$  °C). Erupted lavas are able to flow only during the initial part of the temperature drop, when the system still behaves like a liquid. Thus, emplacement of a lava flow occurs far from thermodynamic equilibrium, as recently acknowledged in works dealing with the syn-emplacement evolution of lava texture and rheology (Chevrel et al. 2013; Kolzenburg et al. 2016, 2017).

Now, if we agree that the emplacement of lava flows occurs when the lava can actually flow, this condition provides the key to identifying the physical boundary of a specific system taken as reference, hereafter termed the *active lava flow system* (ALFS). The ALFS can be defined as the portion of the erupted lava which is connected to the active source of supply and which continues to behave like a liquid (i.e., can flow), constituting the molten fraction of active flow units. The ALFS is clearly an open system evolving in non-equilibrium, because it continuously receives in input mass and energy from the vent (i.e., molten lava and heat advected) and continuously exports mass and energy towards the surroundings as lava cools down through an intermediate viscoelastic condition (James et al. 2004; Hoblitt et al. 2012) and becomes part of the solid “lava deposit” system (Fig. 1).

I ascribe moving, solid crust on the surface of an active lava flow to the “lava deposit” portion of the system, because it

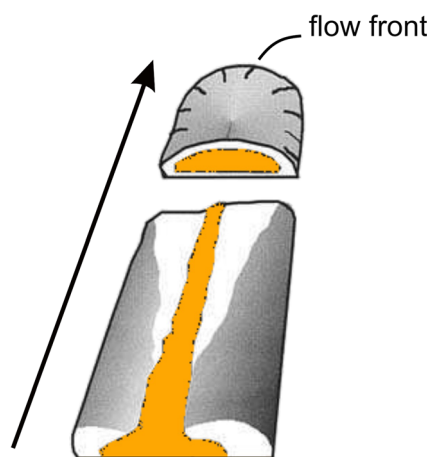


**Fig. 1** Sketch of a channelized flow unit (modified after Kilburn 2000). Only the *orange* part belongs to the ALFS (active lava flow system [hot lava actively flowing]), while *gray* and *white* are made of cooled lava belonging to the lava deposit (e.g., levees and crust). *Black arrow* indicates flow direction

does not actively participate in the flow process, it is just passively transported down flow for a given period of time. The newly formed “lava deposit” is still far from thermal equilibrium with its surroundings and continues to cool by releasing heat into its cooler, surrounding environment (Wooster et al. 1997; Harris 2013 p.261; Coppola et al. 2015). However, the rate of heat dissipation for the “lava deposit” is typically significantly lower than that of the ALFS.

It is possible to define an ALFS to account for the entire mass of lava supplied during an effusive eruption, in which case it is a “total ALFS,” but an ALFS can be defined also for a single flow unit out of many, simultaneously active flow units. In the latter case, it is a “local ALFS” and it “accounts” only for the lava supplied to the specific flow unit (Fig. 2).

An ALFS, just like any other open system, can achieve a non-equilibrium steady or *stationary* state only when *both* the mass budget and the energy budget are zero, i.e., when the rate of input of mass into the system = the rate of output of mass from the system; and the rate of input of energy = the rate of output of energy. In general, a non-equilibrium system in steady state can be a system in which nothing is *physically still* (Fig. 3).

#### The non-equilibrium limit for flow units: the structural relaxation time “ $\tau_s$ ”

In the non-equilibrium framework used here to set current understanding of lava flows, the concept of “flow unit” assumes a specific character. In the present section, I reconsider in detail this crucial item which constitutes the actual *building block* of lava flows (Kilburn and Lopes 1991).

Following the original work of Walker (1971, 1973) regarding lava flow units and the relation between discharge rate and unit length, a general consensus was reached that the relation between the maximum length attained by lava flow unit and discharge rate depends on whether the system is “cooling-limited” or “volume-limited” (e.g., Malin 1980; Guest et al. 1987; Wilson et al. 1993; Pinkerton and Wilson 1994). In the volume-limited case, if the supply stops, then the flow ceases to advance shortly afterwards. Instead, in the cooling-limited case as the flow proceeds downhill, the lava cools and its viscosity increases, higher viscosity means greater “resisting force”, and when the “driving force” (gravity) is eventually balanced, the flow stops advancing even if effusion continues (e.g., Wilson et al. 1993; Harris and Rowland 2009; Castruccio et al. 2013).

However, the dichotomy of volume- vs cooling-limited flow units does not explain the typical flow diversion process, in which a flow unit supplied at a steady rate (and which could apparently keep moving forward), at a given time, breaks its own structure, abandoning a portion of the active flow system, and produces a new flow unit to expand and accommodate the sustained supply. The abandoned portion of the flow unit is

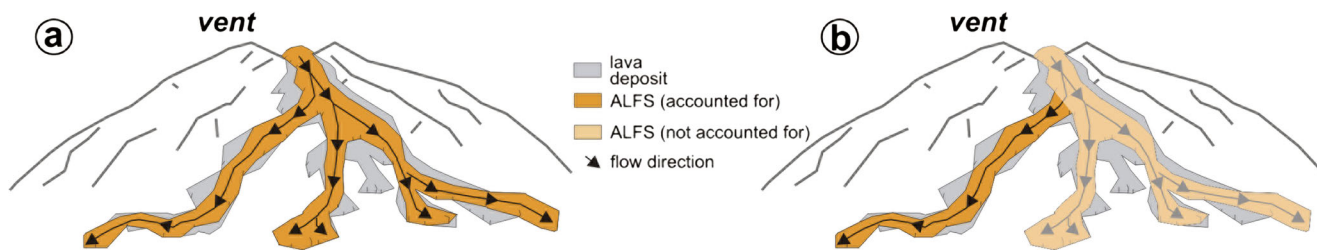


**Fig. 2** Sketch of total (a) and local (b) ALFS. The total ALFS in a accounts for the whole supply and includes all the active flow units.

The local ALFS in b accounts only for the lava supplying the considered flow unit (*bright orange*)

thus “volume-limited,” but this is only a consequence of the real driving factor, which is the diversion process.

Natural diversions in steadily fed and clearly not cooling-limited lava flow units have been described in detail (Tarquini et al., 2012a; Tarquini and de’ Michieli Vitturi 2014), and flow diversions have been reported to occur at a regular pace for long time if conditions remain constant, e.g., “the regular channel switching” over several months during the 2008–2009 Mt. Etna eruption (James et al., 2009). An additional example of a regular duration of lava flow units can be found in the typical emplacement of pillow lavas, characterized by the budding of new units at a relatively constant pace (Jones 1968; Walker 1992), without clear evidence of a cooling limited stop (Moore 1975).

The above points towards the concept of duration (intended as “life span”) as a primary characteristic of lava flow units. The embryo of this concept was already present in the seminal work of Walker (1973), which highlighted that flow units with different initial characteristics (different supply rates, in this case) have a different duration. The concept of life span as a primary characteristic of lava flows is in textbook agreement with the non-equilibrium perspective that is the inspiring idea of the present work. Systems evolving far from the thermodynamic equilibrium are intrinsically characterized by the onset of self-organization structures (also termed “dissipative

structures,” Glansdorff and Prigogine 1971). These structures typically display a characteristic duration and/or characteristic length scale and are well studied in several domains (e.g., Walgraef 1996; Goldbeter 2002; Boekhoven et al. 2015). For example, in the case of volcanic plumes, the far-from-equilibrium nature of the system leads to the formation of specific non-equilibrium dissipative structures (eddies) which are characterized by a given size and duration (i.e., the “eddy turnover time” or “relaxation time”), and these characteristics are linked to specific parameters of the fluid-dynamic system (Esposti Ongaro and Cerminara 2016). For the non-equilibrium perspective proposed here for lava flows, flow units are the relevant dissipative structures (being the analog of eddies), and their duration should be linked to specific parameters of the system.

I here propose that, in the non-equilibrium framework, the default limit in extension of flow units is determined by their limited life span, which is called here structural relaxation time “ $\tau_s$ ” (i.e., the average life span of flow units). However, the relaxation time “ $\tau_s$ ” emerges only when the effusive eruption lasts long enough under relatively stationary conditions (steady supply, constant lava characteristics, etc.) for a duration  $>\tau_s$ . Under these conditions, the non-equilibrium system has the time to arrange itself into fully developed dissipative structures. An example of this process at work in a real lava flows at Mt. Etna is illustrated in the following.

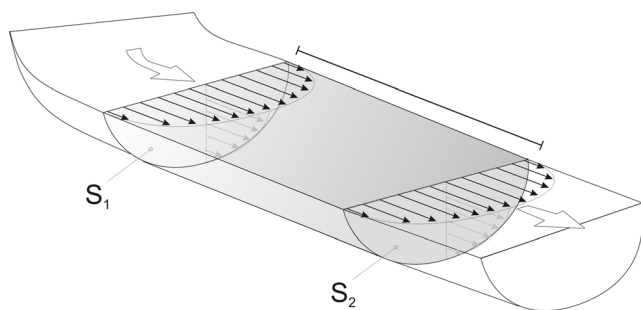


**Fig. 3** An arbitrary segment of a schematic channel between sections  $S_1$  and  $S_2$ , where flow direction is given by the *white arrows*, and *black arrows* give the velocity profile. If the flow is constant (i.e., dynamically stationary), this segment constitutes a non-equilibrium system in steady state having a balanced volume and energy budget (i.e., mass and energy flux in through section  $S_1$  is equal to the mass and energy flux out through section  $S_2$ )

### Mass and energy fluxes in flow units

To understand whether, and if so how, an ALFS can attain a stationary non-equilibrium condition (i.e., if the steady state claimed in the *thermal approach* can apply), the processes responsible for the input and output of mass and energy are considered for two different types of flow unit: a typical “Etnean” channelized flow, where I take that active during the initial phase of Mt. Etna’s 2004–2005 eruption (Burton et al. 2005; Mazzarini et al. 2005; Favalli et al., 2009; Wright et al. 2010; Tarquini et al. 2012a; Coppola et al. 2013; Tarquini and de’ Michieli Vitturi 2014), and a typical “Hawaiian” inflating pahoehoe sheet flow, where considered

sheet flow that formed during the 1986–1991 eruption of Kupaianaha (Mattox et al. 1993; Hon et al. 1994). Both cases have been studied in detail. The Etnean and the Hawaiian cases were fed at comparable discharge rates of  $\sim 2 \text{ m}^3 \text{ s}^{-1}$  for the channelized flow (Mazzarini et al. 2005) and  $\sim 1 \text{ m}^3 \text{ s}^{-1}$  for the sheet flow (Mattox et al. 1993). We can also assume a relatively constant supply in both cases for the time-scales considered here. Lava viscosity at eruption is typically much higher for Etnean lavas than for Hawaiian lavas (Cashman and Sparks 2013), and the slope of the pre-emplacement topography is also different (almost flat for the Kalapana case;  $40^\circ\text{--}10^\circ$  in the Etnean case).

**Mass fluxes**

The mass flux in to each ALFS is comprised of the liquid lava flowing into the flow unit system and is equal to the discharge rate in the Etnean case. The flux of mass out of each ALFS changes according to emplacement style (Fig. 4). In the two test cases, the main mass fluxes out of the ALFS are linked to inflation of the sheet flow or to levee overflow of the channel. In both cases (considering a constant mass input), during the extension of the flow unit downhill, the outward flux of mass can increase up to the point at which the mass budget in the ALFS becomes balanced (i.e., input = output, Fig. 4).

In the emplacement of an inflating sheet flow, the outward flux of mass from the ALFS is due to the transfer of lava from the liquid core to the solid crust (essentially transfer of mass from the ALFS and to the “lava deposit” system). The rate of this transfer is mainly controlled by heat conducted towards the upper surface of the flow (Keszthelyi 1995a; Garel et al. 2015), and heat dissipated into the surrounding environment is

then mostly through radiation (Keszthelyi and Denlinger 1996; Harris et al. 1998; Griffiths 2000; Keszthelyi et al. 2004). The consistent thickness of sheet flows suggests that the inflation process proceeds up to a limiting thickness ( $h_L$  in Fig. 4; Hon et al. 1994; Vye-Brown et al. 2013). Once this limit has been locally attained, inflation ceases and molten lava moves into another part of the system where the inflation process is still active. Hence, the attainment of  $h_L$  causes the actively inflating area to propagate outwards (Fig. 5). The sheet flow, itself, continues to spread through discontinuous breakouts (e.g., Hoblitt et al. 2012). In practice, the rear portion of the flow, where  $h < h_L$ , becomes an extension of the feeder system or “pyroduct” (Coan 1844; Lockwood and Hazlett 2010 p.138), as argued for lava flowing in tubes by Pinkerton and Wilson (1994) and Cashman et al. (1998). Therefore, even if the mass budget is approaching zero, the ideal sheet flow is able to slowly creep ahead and to extend a great distances if supply is sustained (Self et al. 1996; 1998; Thordarson and Self 1998).

The model of Hon et al. (1994; Fig. 6a, c) constrains the initial growth of the inflating upper crust of sheet flows and suggests a concurrent growth of a basal crust (Kauahikaua et al. 1998). However, the rapid growth of a basal crust is not supported by the temperature measurements of Keszthelyi (1995) made at the base of pahoehoe lava lobes and by the field observations of Self et al. (1996, 1998) and Thordarson and Self (1998), who suggest a very low cooling rate at the base of the inflating sheet flows and a limited development of the basal crust. The progression with time of the partition of the incoming volume of lava between lava core and crust (approximate analog of ALFS and lava deposit) is illustrated in Fig. 6b, d. The results of Keszthelyi et al. (2006),

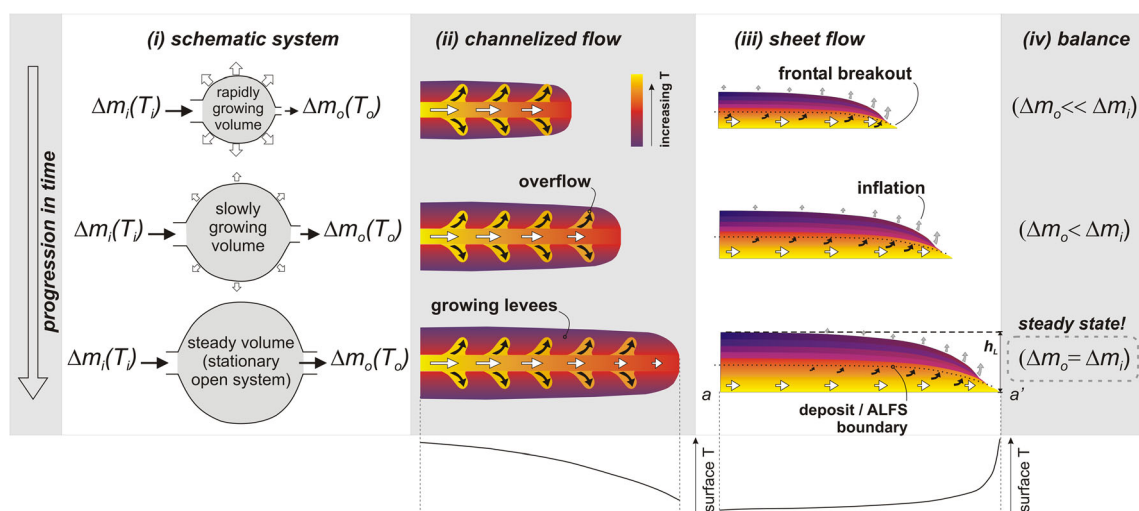


**Fig. 4** Growth towards a steady-state condition for (i) a schematic system; (ii) a channelized system (schematic plan view based on Tarquini et al. 2012a); and (iii) sheet flow system (schematic vertical section based on Hon et al. 2004; Self et al. 1998). White arrows

indicate flow of mass into and through the system; small black arrows indicate directions of mass flow out of the ALFS. Unscaled, downflow approximations of the average surface temperature are given at the bottom of columns (ii) and (iii), while column (iv) summarizes the mass balance

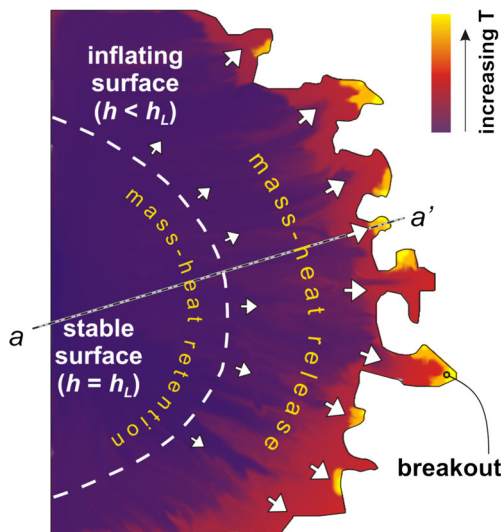


**Fig. 5** Schematic growth of a sheet flow system (plan view). Section *a-a'* is the profile in Fig. 4iii. White arrows indicate directions of flow advance

Self et al. (1996, 1997, 1998), and Thordarson and Self (1998) yield an approximate 1:1 ratio between lava core and crust in mature sheet flows ranging in size from a few meters thick

(Hawaii) up to tens of meters thick (flood basalts in the Columbia River Basalt group) (Fig. 7). The structures observed in the field are the same, irrespective of scale, suggesting that the emplacement mechanisms are similar.

In the case of channelized flows, the main process responsible for the outward flux of mass from the ALFS is mechanical, i.e., from repeated overflows removing lava from the active channel. This process drives the growth of solid levees and has been widely documented in lava flows at Mt. Etna (Sparks et al. 1976; James et al. 2007; Tarquini and de' Michieli Vitturi 2014), in other terrestrial volcanoes such as Mauna Loa and Kilauea (Hawaii, Moore 1987; Cashman et al. 2006; Harris et al. 2009), and has also been inferred in Martian lava flows (Glaze and Baloga 1998; Glaze et al. 2009). In this case, in contrast with the case of the inflating sheet flow, lava removed from the system can still be liquid (e.g., James et al. 2007).

In recent years, new remote sensing technologies allowed the acquisition of short time interval time series of topographies of active lava flows (e.g., Favalli et al. 2009, 2010; Wadge et al. 2011, 2012). Analysis of similar data allowed the identification and quantification of the pulsating dynamic responsible for the onset of iterative overflows both in basaltic

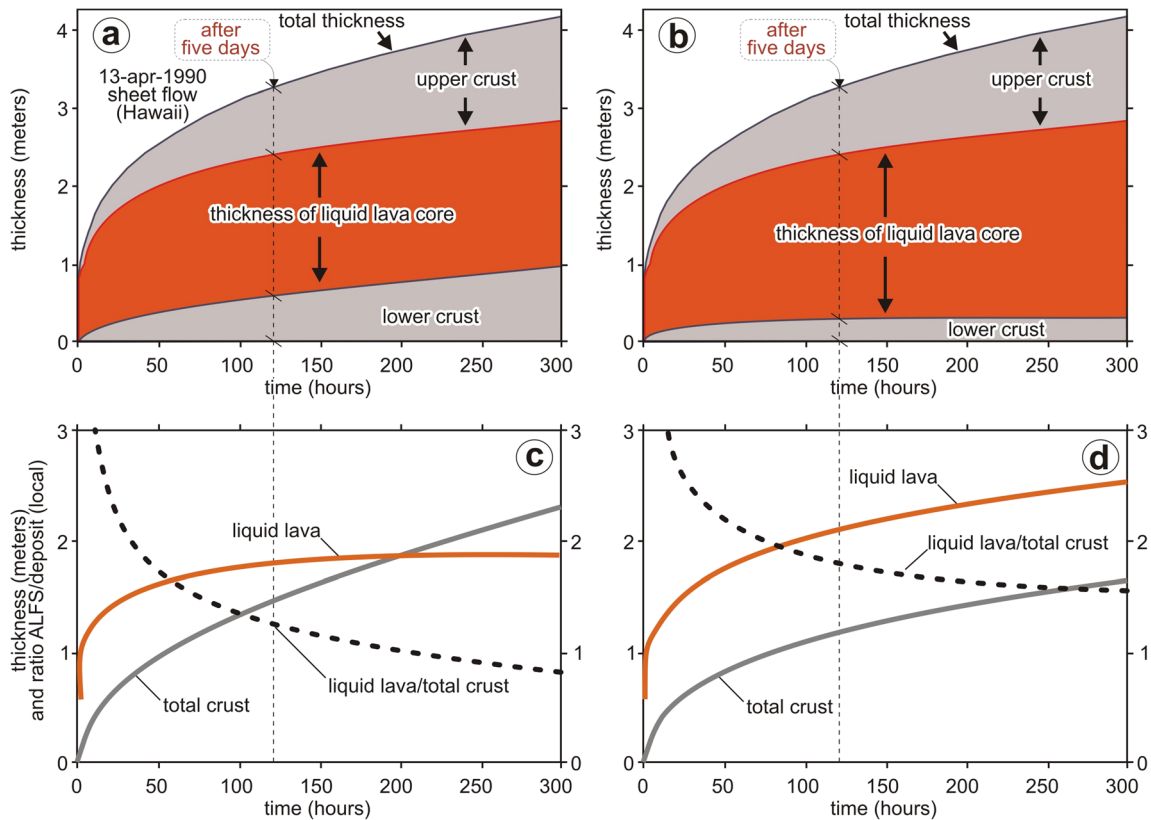
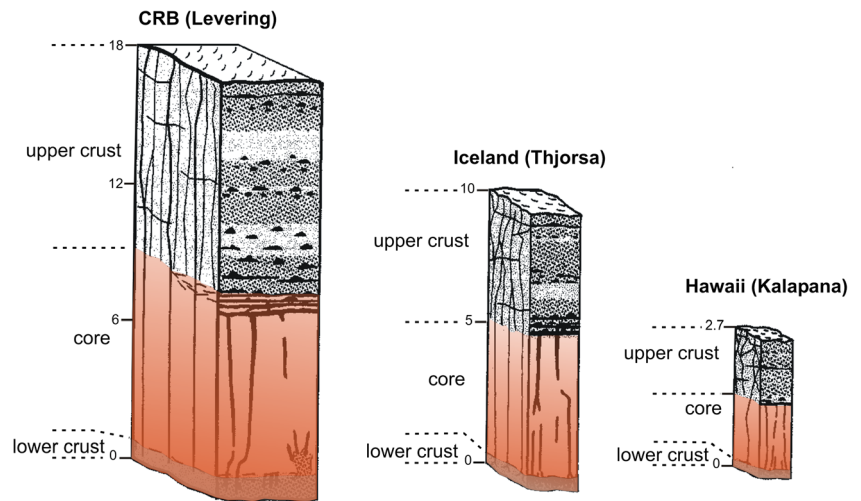


**Fig. 6** Partition of lava between the liquid lava core and the crust in a sheet flow. **a** Sketch of the progression of the inflation process redrawn after Hon et al. (1994). **b** As **a**, but graphically modified to represent the formation of a thinner basal crust in agreement with Self et al. (1998). **c**

Measurements of the thicknesses and local ratio (i.e., along vertical lines identifying a given time horizon) between the ALFS and deposit sketched in **a** for increasing time. **d** As **c**, but for the sketch in **b**

**Fig. 7** Cross sections of inflated pahoehoe flows in Hawaii, Iceland, and the Columbia River Basalts (CRB) showing the ratio of upper crust, core, and basal crust. Thicknesses are in meters (modified after Thordarson and Self 1998). See Harris et al. (2017) and references therein for details about the fine structures inside each vertical division (e.g., multiple vesicular zones in the upper crust, *dotted*)



channelized flows (Favalli et al. 2010, Fig. 8) and in more acidic channelized lavas (Wadge et al. 2012).

Short time interval time series such as the one acquired by Favalli et al. (2010) are rarely available. However, through a specific LIDAR data processing technique, a pulsating behavior similar to the one in Fig. 8 has been assessed also in the 2004 lava flow unit considered here as test case (Favalli et al. 2009). The morphometric analysis of Tarquini et al. (2012a) and Tarquini and de' Michieli Vitturi (2014) further showed that a single high-resolution topography can provide systematic downflow measurements of the cumulative volume of lava constituting the flow field (irrespective of actively flowing liquid or lava deposit), with details for single flow units (Fig. 9).

Tarquini and de' Michieli Vitturi (2014) also showed that, by combing morphometric data with additional observations

(e.g., Wright et al. 2010), it is possible to infer the local partition of the lava volume between lava deposit and ALFS (Fig. 10). Those authors illustrated that a lava channel tends to maintain a constant sectional area through time (i.e., a constant maximum volume of liquid lava contained, Fig. 10c), while the thickness of the “lava deposit” system (or the relative volume per unit length) increases substantially as a result of repeated, rapidly quenched overflows (Sparks et al. 1976). Figure 10c shows that in 5 days the local volume ratio ALFS/deposit decreased from ~1:2 to ~1:10, highlighting the extremely high rate of mass dissipation (i.e., rate of mass transfer from the ALFS to the deposit per unit length of flow unit) in channelized flows.

In both types of flow unit, the total mass of the ALFS increases with time as the flow unit grows (Fig. 4) and decreases when a diversion cuts the supply to a given branch of

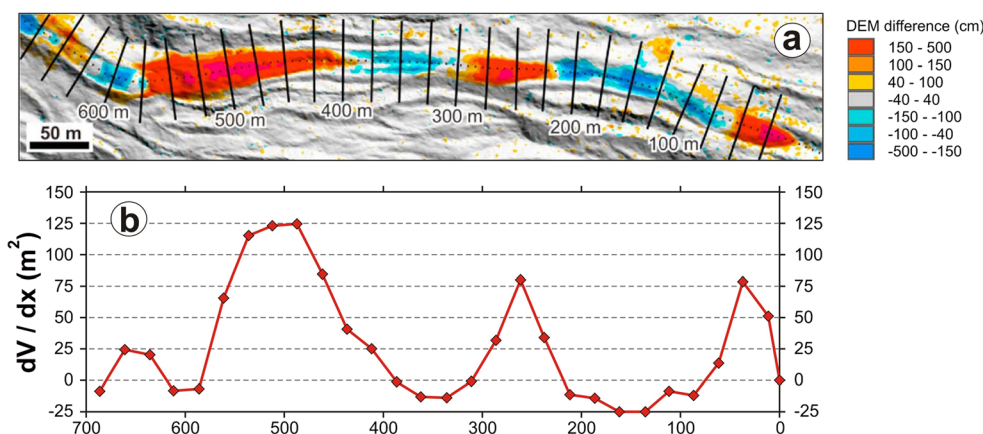


**Fig. 8** Example of lava pulses measured through the processing of a time series of LIDAR DEMs during the 2006 eruption at Mt. Etna (modified after Favalli et al. 2010). **a** DEM difference map showing the changes in elevation over a time interval of ~2.5 h, along the terminal ~700 m of a channelized flow unit; *red hues* highlight a rise in the lava level (i.e., an increase in elevation) and *blue hues* a draining channel (i.e., a decrease in

elevation). **b** Plot of the volume difference (in the time interval) within flow unit sectors between adjacent cross-sections (*black lines*) in **a**, expressed as volume change per unit channel length. Three large pulses advancing downflow are evident (Favalli et al. 2010), as well as the piling-up of lava onto levees

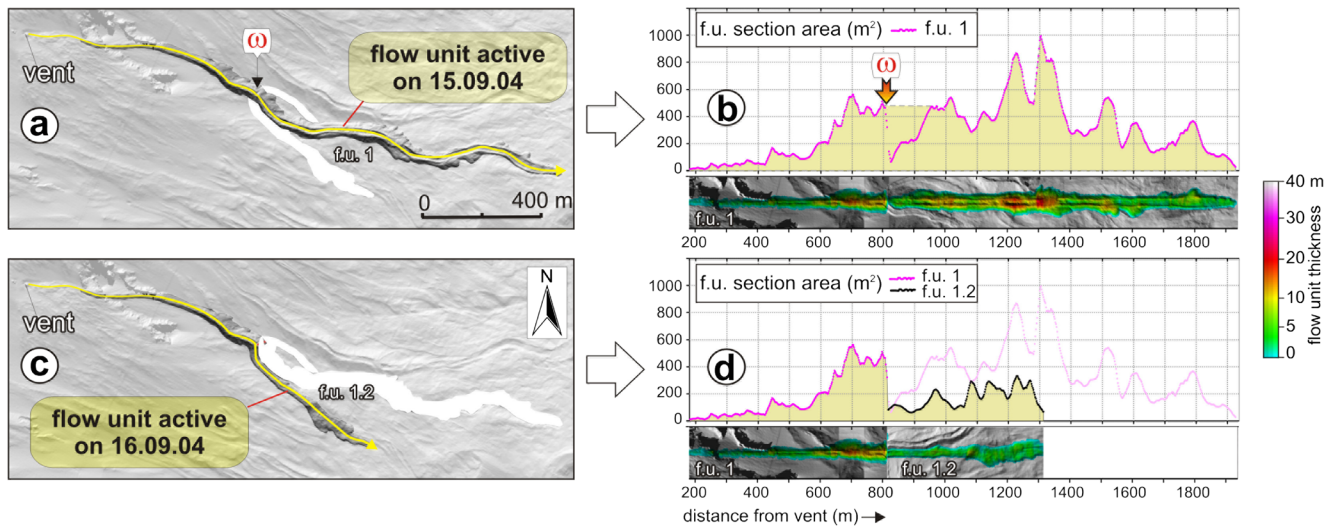


**Fig. 9** Flow units active during the initial phase of the Mt. Etna 2004–2005 eruption with relative downflow quantification of cross-sectional area. In **a** and **c**, the flow units active on 15–16 September 2004 (respectively) are mapped on the LIDAR-derived topography (Mazzarini et al. 2005), with white masks hiding the flow units active in different days. **b** and **d** show the downflow measurements of cross-sectional for **a** and **c**, respectively, obtained by systematic processing of

elevation profiles (Tarquini et al., 2012a, b). This processing also allows derivation of downflow thickness and volume (see also Fig. 10). A shaded relief image of the flow unit projected in an along flow coordinate system is aligned below the plot in **b** and **d**, with color-coded indicating flow unit thickness (see Tarquini et al. 2012a and Tarquini and de' Michieli Vitturi 2014 for further details). The label “ $\omega$ ” indicates the diversion point (i.e., a flow unit relaxation)

the flow field (e.g., Fig. 9). In this case, the portion of the flow for which supply is cut becomes inactive and the relative mass of liquid lava is released from the ALFS and becomes lava

deposit. The surface of this newly formed lava deposit now cools rapidly, being not rejuvenated anymore by internal motion.

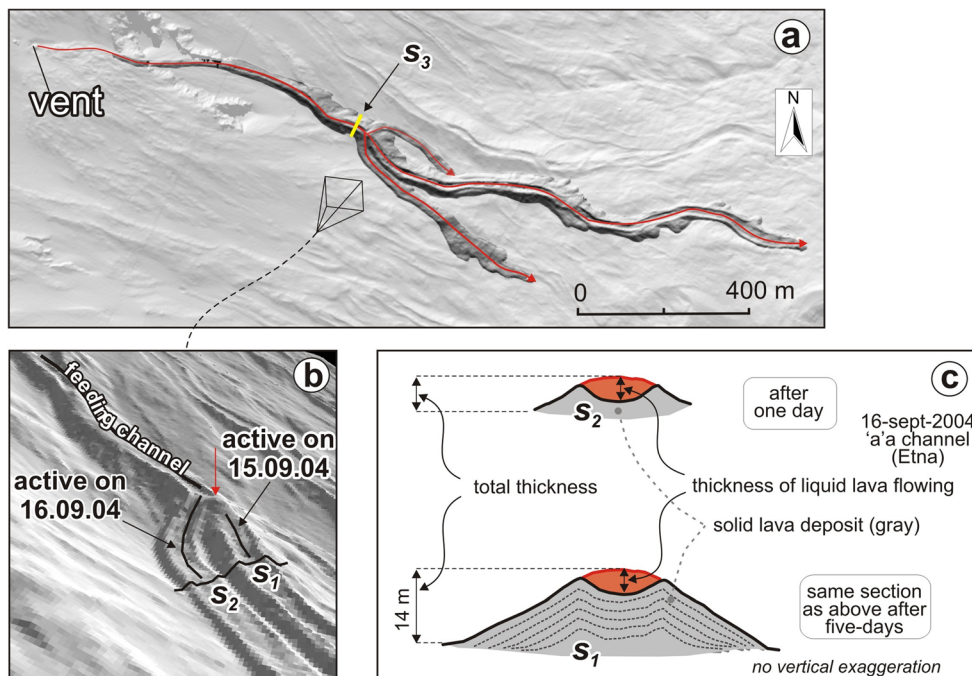


**Fig. 10** Morphology of lava channels from the 2004 LIDAR survey at Mt. Etna. **a** Plan view with axis of the three branches of the flow (section  $S_3$  is used in Fig. 15). **b** 3D view of the diversion point with indication of the sections  $S_1$  and  $S_2$  which yields the elevation profiles in **c**; red arrows indicate a bulge which appears to block the flow towards the previously active channel (Tarquini and de' Michieli Vitturi 2014). **c** Elevation

profiles of sections  $S_1$  and  $S_2$  in **b** with schematic progressive stacking of lava layers to increase the deposit thickness, and local partitioning of the erupted lava volume between liquid ALFS (represented by the orange cross-sectional area) and solid “lava deposit” (represented by the gray cross-sectional area): see Tarquini and de' Michieli Vitturi (2014) for details



The above description of the evolution of the two types of flow units clarifies that, for any given discharge rate, the rate of mass dissipation per unit length from the ALFS is much higher in a channelized flow than in a sheet flow. If supply is maintained, a sheet flow can slowly evolve towards a long-standing, well-insulated, quasi-steady-state ALFS, which can attain large distances. A channelized flow is, instead, a highly dissipative system that rapidly transforms the ALFS into a thick lava deposit. The ALFS portion is typically higher than the lava deposit portion in an active sheet flow, and the opposite is true in an active channelized flow unit due to the rapid turnover of lava constituting the ALFS. In Fig. 11, the progression with time of the volume ratio ALFS/deposit (equivalent to the ratio between the relative section areas) is plotted for both types of flow unit. For the sheet flow, values are obtained by measuring in Fig. 6a the areas of liquid lava core and crust (alias ALFS and deposit) at increasing time intervals (i.e., between  $t_I = 0$  and  $t_x$ , with  $t_x$  varying between 0 and 300). For the channelized flow, instead, the progression with time of the ratio ALFS/deposit is inferred from the layout of measurements of channel dimensions and deposit presented in Tarquini et al. (2012a) and Tarquini and de' Michieli Vitturi (2014), and summarized here in Figs. 9 and 10.

In principle, when steady-state conditions are attained, if one considers only the flow front, both lava units in Fig. 4 would appear physically motionless, because the flow front cannot advance any further. The mechanisms associated with continued mass flux are, instead, fully active behind and up flow from the front. I note here that this situation coincides with the “stopping condition” defined by Baloga et al. (1998) and by Glaze and Baloga (1998).

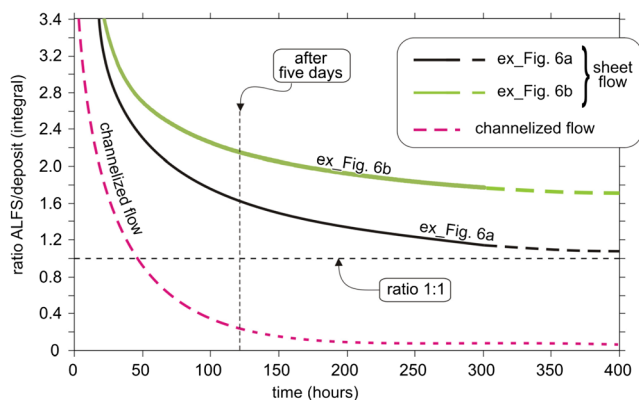


**Fig. 11** Evolution with time in partitioning of the erupted lava between the ALFS and lava deposit for the two types of flow unit considered. For the sheet flow, both the local partitions illustrated in Fig. 6a, b between crust (as an approximation of the lava deposit) and liquid core (as an approximation of the ALFS) have been integrated over time to obtain the solid black curve and solid green curve, respectively; black and green dashed lines are the inferred prolongation beyond 300 h. For the channelized flow, the magenta dashed line is derived as explained in the main text, and the dotted line is its inferred continuation (beyond 5 days)

### Energy fluxes

As a first approximation, the total energy involved in the emplacement of a lava flow is composed of potential energy ( $U$ ) and heat ( $Q$ ). Potential energy ( $U = mV_g$ , where  $V_g$  is the gravitational potential and  $m$  is the mass) is transformed into kinetic energy as the fluid flows downhill and into thermal energy by viscous heating. For a portion of the flow, the potential energy available during emplacement ( $\Delta U$ ) can be written as

$$\Delta U = m g \Delta h \tag{1}$$

where  $g$  is gravity and  $\Delta h$  is the elevation difference between the source and the elevation at which the mass stops (at this point,  $m$  moves from the ALFS to the “lava deposit” system). In the case of basaltic lava, Eq. (1) yields  $\sim 2 \times 10^4$  J per cubic meter of lava per meter of elevation change ( $\Delta h$ ). The average  $\Delta h$  for basaltic lavas erupted at Mt. Etna is about 700 m (Tarquini and Favalli 2011), which implies  $\Delta U \sim 1.4 \times 10^7$  J per cubic meter of lava. Instead, average  $\Delta h$  for the lava erupted at Holuhraun (Iceland) during 2014–2015 (Gudmundsson et al. 2016; Pedersen et al. 2017) was 100 m, yielding  $\Delta U \sim 2 \times 10^6$  J per cubic meter of lava.

The energy available as heat ( $\Delta Q$ ), neglecting latent heat of crystallization (Dragoni and Tallarico 2009), is

$$\Delta Q = m c_p (T_i - T_o) \tag{2}$$

where  $c_p$  is specific heat ( $J \text{ kg}^{-1} \text{ K}^{-1}$ ), and  $T_i - T_o$  is the temperature difference between the eruption temperature  $T_i$  and the temperature  $T_o$  at which the lava with mass  $m$  exits the ALFS. I note that  $\Delta T (T_i - T_o = \Delta T)$  is the equivalent to the difference between the eruption temperature, and the temperature at which “flow stops moving” in the model of Pieri and Baloga (1986). By using standard values of  $c_p$  for basaltic lava at eruption temperature (e.g., Coppola et al. 2013), we obtain  $\Delta Q \sim 2 \times 10^6$  J per cubic meter of lava per degree centigrade of cooling (Fig. 12). Thus, the energy released by the ALFS is at least one order of magnitude greater than the potential energy available and can be up to two orders of magnitude greater, or more, if lava moves over flat ground, as in the Holuhraun case. Thus, the energy budget of an ALFS is dominated by heat advected into the system during the inward flux of mass. Heat then advects out of the ALFS by the transfer of mass to the “lava deposit” system

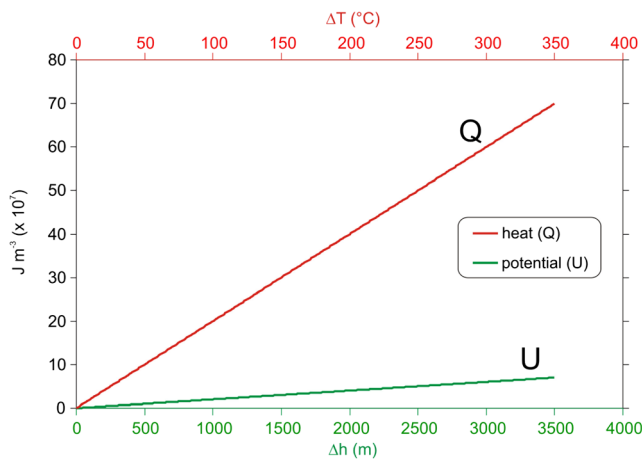


**Fig. 12** Heat and potential energy for given  $\Delta T$  and  $\Delta h$ . For the calculation of  $Q$ , a constant  $c_p$  is assumed, although  $c_p$  can vary with temperature (e.g., Dingwell 1998). I assume eruption temperature to be stable

and, thus, by heat loss to the surroundings through radiation and/or convection.

### Transient term in the thermal budget

While the inward flux of mass per unit time ( $\Delta m_i/\Delta t$ ) into the ALFS comprises molten lava effused from the source at temperature  $T_i$ , the outward flux of mass per unit time ( $\Delta m_o/\Delta t$ ) comprises cooled lava at temperature  $T_o$  which is transferred to the “lava deposit” system. For an ALFS evolving under a constant supply rate ( $\Delta m_i/\Delta t = \text{const.}$ ), heat advection into the system by the input mass is  $Q_{\text{adv-in}}/\Delta t = (\Delta m_i/\Delta t) c_p (T_i)$ , and heat advection out of the system by the output mass is  $Q_{\text{adv-out}}/\Delta t = (\Delta m_o/\Delta t) c_p (T_o)$ . Thus, a heat budget of the open ALS can be written as

$$\left(\Delta m_i/\Delta t\right) c_p (T_i) = \left[ (\Delta m_i - \Delta m_o) / \Delta t \right] c_p (T_x) + \left(\Delta m_o/\Delta t\right) c_p (T_o) + Q_{\text{rad}}/\Delta t \quad (3)$$

Here,  $Q_{\text{rad}}$  is the heat released by radiation, which dominates the heat budget in subaerial environments (Keszthelyi and Denlinger 1996; Harris et al. 1998; Griffiths 2000; Keszthelyi et al. 2004), and  $T_x$  is the temperature of the ALFS (averaged over its entire volume  $T_i > T_x > T_o$ ).  $Q_{\text{rad}}/\Delta t$  balances the heat advected out of the ALFS by  $\Delta m_o/\Delta t$ . However, Eq. (3) is difficult to solve because, assuming  $\Delta m_i/\Delta t$  and  $T_i$  can be evaluated by direct measurement (Harris et al., 2007a, b, c), the measurement of both  $\Delta m_o/\Delta t$  and  $T_x$  is highly impractical, and thus, two variables are unknown. In any case, as time elapses, the mass budget approaches zero, so that eventually  $\Delta m_o = \Delta m_i$  (Fig. 4). At this point, the first term

on the right-hand side of Eq. (3) vanishes, and the standard simplified equation of the “thermal proxy” is obtained:

$$Q_{\text{rad}}/\Delta t = (\Delta m/\Delta t) c_p (T_i - T_o) \quad (4)$$

where  $\Delta m$  is equal to the lava supplied to the ALFS ( $\Delta m_i$ ), or released from it (because  $\Delta m_i = \Delta m_o$ ) per unit time, and  $T_i$  is the temperature of lava entering the ALFS and  $T_o$  is that of lava exiting the ALFS. Equation (4) is now equivalent to empirically derived thermal proxies formulated elsewhere (e.g., Harris and Baloga 2009; Coppola et al. 2013). In natural cases,  $Q_{\text{rad}}$  can be retrieved through thermal remote sensing techniques (e.g., Ganci et al. 2011; Ramsey and Harris 2012; Harris 2013; Coppola et al. 2015); eruption temperature and  $c_p$  are known;  $T_o$  can be estimated by considering rheological, thermal, and flow dynamic regime of the lava involved (Harris and Baloga 2009). Hence, Eq. (4) can be solved and provides a straightforward way to approximate lava supply rate to the ALFS. The first term of the right-hand side of Eq. (3) expresses a previously “hidden” transient term in the standard formulation of the thermal budget which, in the form given here, assumes a “dynamic” state, as opposed to the classic “static” state (e.g., Garel et al. 2015).

After exiting the ALFS, the lava continues to cool, releasing additional heat ( $Q_{\text{add}}$ ). This term is not considered in either Eqs. (3) and (4), because it is not part of the ALFS. However, the cooling rate of the “lava deposit” system decreases rapidly to a much lower value than that of the ALFS, because the radiative power is proportional to the fourth power of the surface temperature, so that heat losses reduce following a power law as the temperature decreases (e.g., Keszthelyi et al. 2004; Harris et al. 2007a; Harris 2013).

### The influence of slope

Gravity determines the force driving the flow downhill ( $F = m g \sin(\theta)$ , where  $\theta$  is the slope), so that the slope of the topography strongly influences the evolution of the ALFS (Miyamoto and Papp 2004; Favalli et al. 2009, 2012b). A steeper local slope will mean that a greater force  $F$  is applied to the flow. All the other factors being equal, a greater shear stress induces higher strain rates, leading to faster and thinner flow units (e.g., Hulme 1974). To conserve volume, thinner flow units will have a higher surface area  $A$  ( $A = V/h$ , where  $h$  is the flow thickness), which means a higher surface dissipating heat towards the surroundings (Robertson and Kerr 2010).

The above relation between slope and flow surface area applies for dispersed flows, i.e., for lava flows which do not form levees. When flowing lava becomes constrained into a channel by the formation of levees, instead, the situation is reversed, with an increase in slope promoting a narrower channel in which a

thicker and faster flow moves downhill (Kerr et al. 2006). However, a faster flow tends to disrupt the lava crust more easily, exposing a higher fraction of the hot core (Rothery et al. 1988; Harris and Rowland 2001; Cashman et al. 2006), and a higher elevation gradient (combined with higher velocity) also promotes systematic overflows iteratively spreading thin blankets of hot lava over the levees (James et al. 2007; Tarquini and de' Michieli Vitturi 2014). The latter point is in agreement with the direct correlation between slope and heat dissipation observed in channelized lava flows at Mt. Etna (Wright et al. 2010; Lombardo 2016). Thus, although the interplay between flow velocity and heat release appears rather complex, the overall result seems that a steeper slope promotes a higher rate of heat dissipation per unit volume of ALFS.

### Lava flow advance, flow unit relaxation, and steady state

Figure 13 gives examples of pseudo-steady state in open, non-equilibrium ALFSs, observed for idealized simulations, analog experiments, and natural lava flows. In the analog experiments of Garel et al. (2014), once a pseudo stationary state is attained, minor fluctuations occur due to cycles of stagnation and overflow (O1, O2, and O3 in Fig. 13b). The overflows promote rapid spreading of the hot, molten wax (i.e., the ALFS), which results in a sudden increase in radiative power. The ALFS area during the initial phase of the 1991–1993 eruption at Mt. Etna (Fig. 13c) indicates that a stationary state was attained after about 3 weeks. Figure 13d illustrates that power radiated during the initial phase of the 2004–2005 eruption at Mt. Etna also reached a steady state after about 3 weeks (data from Coppola et al., 2015).

A combined analysis of Fig. 13d, e further provides a good example of the structural relaxation process at work. The sudden decrease D1 in the trend of the radiative power in Fig. 13d occurred the same day as the natural diversion in Fig. 13e. Tarquini and de' Michieli Vitturi (2014) described in detail this diversion from a morphological point of view, highlighting that the lava flow in question was neither cooling- nor volume-limited. The event D1 constitutes an ideal case of structural relaxation of a channelized lava flow. Considering that the supply rate during the time considered in the whole plot is essentially constant (Tarquini and de' Michieli Vitturi 2014 and references therein), the cause-effect relation between a diversion (or relaxation) and a decrease in radiative power provides a key to interpret all the other sudden decreases in the trend of the radiative power in Fig. 13d as structural relaxations of flow units that form an increasingly braided flow field (James et al. 2006, 2007).

Figure 13d further illustrates that the lava channel structure relaxed twice well in advance the attainment of a quasi-steady state (diversions D1 and D2). If we

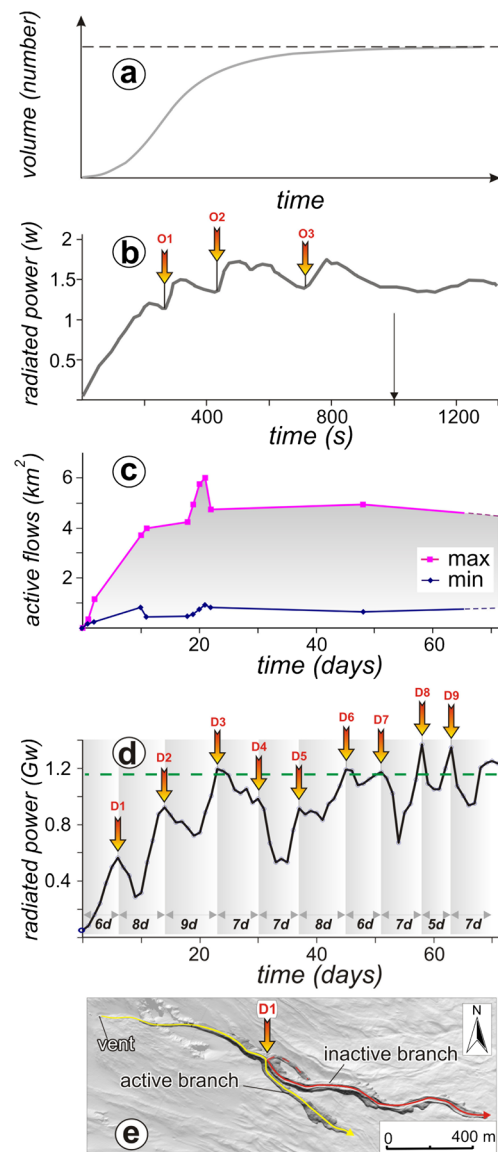


**Fig. 13** Growth of non-equilibrium open ALFS to reach a pseudo-steady state. **a** Typical logistic curve for a system expanding against an external constraint (e.g., growth of a population, Gresham and Hong 2015). **b** Radiative power recording during spreading of PEG wax at constant supply (from Garel et al. 2014); the radiated power is a proxy of the extent of the active area, and also of the active volume (Garel et al. 2014). **c** Area of active lava flows during the initial 2 months of the 1991–1993 effusive eruption at Mt. Etna, (from Harris et al. 1997). **d** Volcanic radiative power (3 points running average) during the initial 2 months of the 2004–2005 effusive eruption at Mt. Etna (from Coppola et al. 2013; 2015); green dashed line represents the pseudo-stationary state. **e** Lava flow field mapped from a 16 September 2004 LIDAR survey (Mazzarini et al. 2005) with diversion point D1 marked; red and yellow lines are the axis of inactive and active flow units (respectively) at the time of the survey

consider the time interval between all the relaxations, we find that a relatively regular average structural relaxation time of  $\sim 7$  days applies. Such a steady frequency suggests a fully developed dissipative structure.

In terms of the ALFS, a flow diversion (or structural relaxation) resets the system further from its maximum extension (Fig. 4). The closer to the vent the diversion occurs, the more radical the consequent decrease in radiative power. For example, Fig. 9d shows that diversion D1 occurred about 800 m downhill from the vent and caused the radiative power to be reset at about one fourth the maximum power attained later (Fig. 13d), while D3 and D6 (on the basis of the thermal signal alone) arguably occurred in distal reaches, explaining why they caused only a small decline in the total radiative power.

The concept of structural relaxation in flow units becomes clearer through a comparison with the structural relaxation ruling the behavior of liquids (including silicate melts). The relaxation time “ $\tau_\alpha$ ” of liquid microstructure is linked to the liquid viscosity  $\eta$  by the relation  $\eta \propto \tau_\alpha$  (Dingwell and Webb 1989, 1990; Cavagna 2009). In the microscale system, the structural relaxation is effectively illustrated by the “cage effect” (Fig. 14), namely the transient trapping of atoms or molecules by their neighbors (e.g., Champion et al. 2000; Larini et al. 2008). The trapped particle is not immobilized by the surroundings, but undergoes fast irregular vibrations having a given average amplitude  $r$ . After an average time  $\tau_\alpha$ , the cage constraints weaken, due to the rearrangement of the surroundings, and the trapped particle is released (e.g., Ottochian et al. 2012). It is exactly the occurrence of the release step which makes the difference between a solid, in which the structural

cage never gives up, and a liquid (or even a glass), in which the structure relaxes after a given time, so that the mass can flow. A higher temperature increases the particle oscillation, and this explains why  $\tau_\alpha$  is reduced, as is the liquid viscosity, in hotter liquids.

In the macroscale dissipative structure constituted by a channelized flow, the cage effect is exerted by the levees, which constrain the expansion of the flow along a given track, while the particle oscillation (causing the so-called cage wobbling) is represented by the typical pulsating behavior of the lava flux in the channel (e.g., Favalli et al. 2010; Wadge et al. 2012; Fig. 8), which leads to overflows and a thickening lava deposit. The growing deposit, in turn, constitutes an evident “rearrangement of the surroundings.” As time elapses, a lava channel strongly modifies the pre-existing topography becoming a “perched flow” (Patrick et al. 2011) in some cases (Fig. 10c). In practice, what was a local topographic minimum when the flow unit found its way downhill becomes later a local maximum which destabilizes the original path (Fig. 15). Well in advance the current era of high-resolution topographies, Frazzetta and Romano (1984), in reporting about the 1983 Mt. Etna eruption, already argued that “almost continuous oscillations in effusion rate (...) seem to have played a prominent role in the morphological modifications of the main lava channel” (Frazzetta and Romano 1984).

As time passes, the endurance of levees is repeatedly tested by pulses of lava and rafted crust (James et al. 2007) and by other complexities occurring during emplacement such as flow blockages (Lipman and Banks 1987; Guest et al. 1987; Bailey et al. 2006; James et al. 2012), so that levee breaching becomes increasingly probable. Thus, the duration of similar channelized flows is intrinsically limited by their own emplacement dynamics. The stronger the pulses in the channel (i.e., the higher the oscillation of the structure), the lower the structural relaxation time  $\tau_s$ . A higher slope facilitates the overflow dynamics and, thus, promotes a lower  $\tau_s$ .

The above explanation of the structural relaxation of flow units suggests why sheet flows have typically a much higher structural relaxation time  $\tau_s$  than channelized flows. Sheet flows have been observed withstanding significant supply variations and last for months (Mattox et al. 1993, Kauahikaua et al. 1998), and they appear to stop essentially when the upstream supply has been definitely diverted (unless other main constraints such as a topographic confinement applies), perhaps for reasons not related to the dynamic of the sheet flow itself but rather to the feeding system. Sheet flows are arguably subject to the same variations in the supply rate which trigger the formation of pulses in channelized flows (Favalli et al. 2010; Tarquini and de’ Michieli Vitturi 2014), but they tend to have a much larger ALFS volume than equally fed channelized flows (Fig. 11) and progress downhill along a wider, dispersed flow front. This difference implies a higher inertia and an inherently stable structure which is apparently able to damp the incoming fluctuations in lava flux.

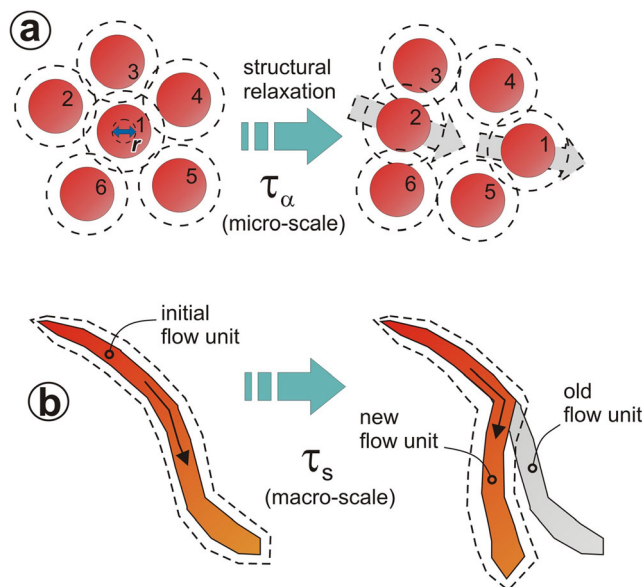


**Fig. 14** Structural relaxation in the microscale structure and in the macroscale structure. **a** The cage effect in viscous liquids. After an average time  $\tau_\alpha$ , the restraint weakens, the trapped particle “1” escapes from the cage and is replaced by a new one, “2” (modified after Ottochian et al. 2012). **b** Structural relaxation of a channelized lava flow. After an average time  $\tau_s$ , the continuous modifications of the surroundings due to the flow dynamics weaken the cage effect exerted by the levees, and an old branch becomes inactive while a new one forms

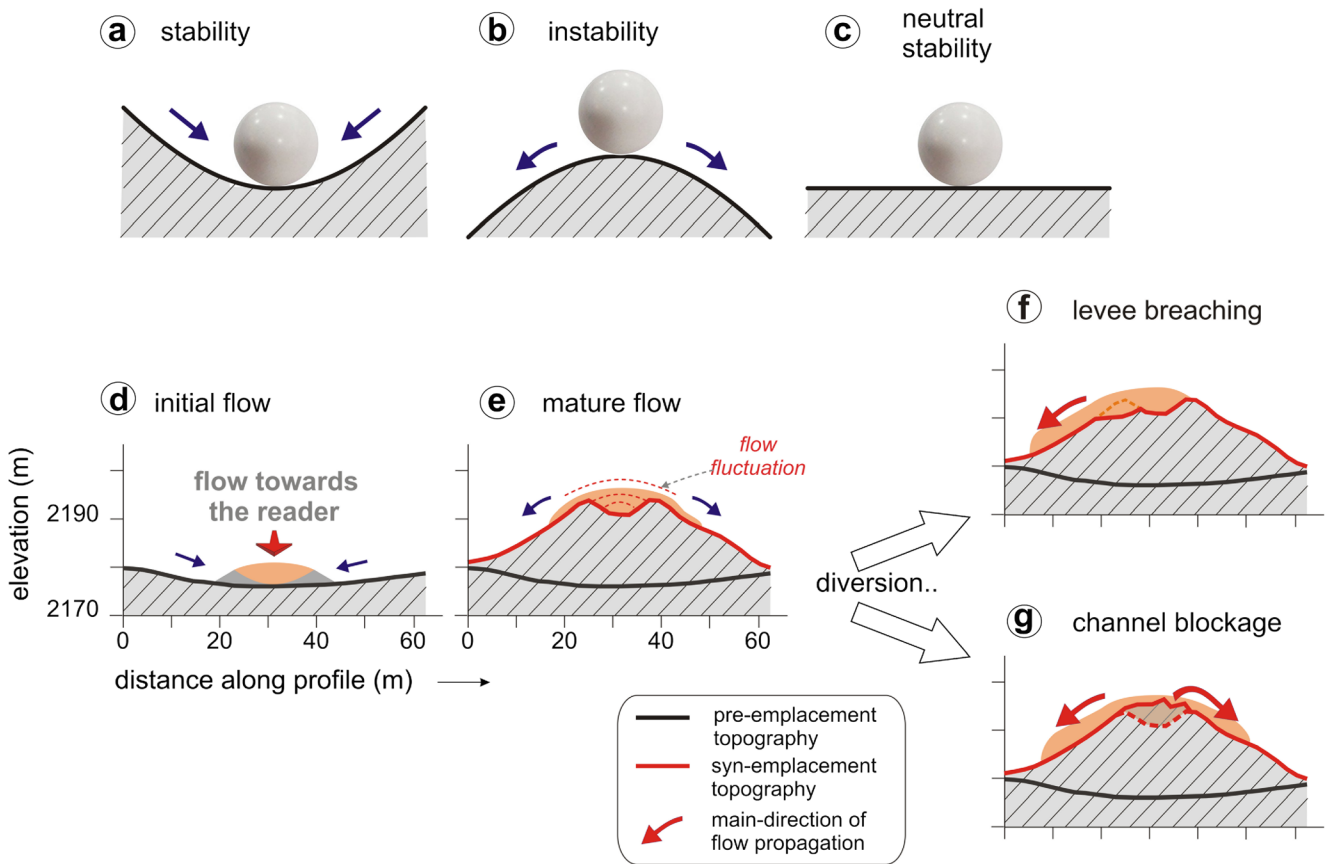


**Fig. 15** Sketches of mechanical stability, instability, and neutral stability, which have similarities with the evolution of the topographic constraint during emplacement of a channelized flow. *Dark blue arrows* indicate the direction of the constraint in the vicinity of the ball or of the lava flow with respect to the planar section. **a** Stability: the ball can withstand small perturbations and reverts to the original position. **b** Instability: the ball cannot revert to the same position if perturbed. **c** Neutral stability: the constraining floor has no effect on the ball. **d** Existing topography drives the flow towards the pre-emplacment steepest descent path which constitutes a local attractor (the sketch of the very early flow here is

hypothetical). **e** After 5 days of ongoing emplacement, the thick lava deposit altered substantially the former stability of the original path in **d**, and the situation is now similar to **b**; in these conditions, a permanent diversion occurs when the constraint of the levees is definitely overwhelmed. Profiles in **d** and **e** are the real pre- and syn-emplacment topography along section S<sub>3</sub> in Fig. 10a (i.e., the TINITALY DEM of Tarquini et al. 2012b, and the LIDAR DEM of Mazzarini et al. 2005, respectively). **f** and **g** illustrate a relaxation through levee breaching or channel blockage (respectively)

### Electric, gravity, and lava currents

Analogies between electric circuits and more complex processes occurring in natural systems are quite common (e.g., Patrick et al. 2004; Kleidon 2010), and I propose that an analogy exists between ALFS and electric currents. The following relations summarize the main fluxes of energy involved in different kinds of stationary currents: an electric current, a gravity current, and a lava “current”:

$$P_E = (\Delta C / \Delta t) \Delta V_E \tag{5}$$

$$P_G = (\Delta m / \Delta t) \Delta V_G \tag{6}$$

$$P_H = (\Delta m / \Delta t) c_p \Delta T \tag{7}$$

For Eq. (5),  $P_E$  is electric power (in watts),  $\Delta C / \Delta t$  is the electric current, and  $\Delta V_E$  is the variation in electric potential.

For Eq. (6),  $P_G$  (in watts) is the gravitational energy released per unit time, and  $\Delta V_G$  is the variation of the gravitational potential ( $\Delta V_G = g \Delta h$ ). In Eq. (7),  $P_H$  (in watts) expresses the heat released by the lava flow per unit time. Equation (5) applies to an electric circuit where a power supply (e.g., a battery) provides a constant potential difference  $\Delta V_E$ , and a flow of electric charge  $\Delta C / \Delta t$  develops through a conductor having a resistance  $R$ . A similar system is described by Ohm’s law, where  $\Delta V_E$  written in full is  $RI$ ,  $I$  being the electric current (Fig. 16a).

Equation (6) expresses the power required to maintain a steady gravity current at mass flux  $\Delta m / \Delta t$  as it descends a vertical height of  $\Delta h$  (Fig. 16b). When the gravity current spreads over a flat area (i.e.,  $\Delta h = 0$ ), the energy budget of the system evolves, now being a function of kinetic energy and pressure driving the current away from the source (Fig. 16c). The device maintaining

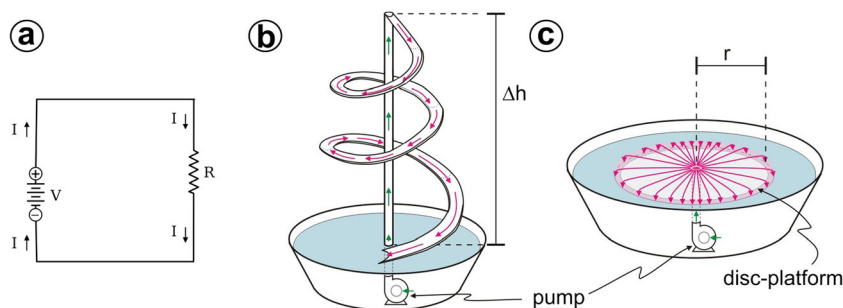


**Fig. 16** Examples of stationary currents. **a** Electric current in a simple circuit where energy flow is governed by Ohm's law,  $V = RI$ . **b** Gravity current expressed in terms of a liquid flowing down an open channel driven by hydrostatic pressure acting over height  $\Delta h$ . A pump provides

the necessary power to close the circuit maintaining the stationary current. **c** Gravity current on a flat platform (with radius  $r$ ) lying at the same level of the liquid in the basin. As in the case of **b**, a pump maintains the gravity current under stationary conditions

the flux at the source (the pumps in Fig. 16) is analog of the battery in the electrical current case.

Equation (7) expresses the heat released by a lava current (in the absence of viscous heating and latent heat of crystallization). It only applies when a lava flow, evolving under a constant supply, attains steady-state conditions (i.e., when both the mass and the heat budgets balance). In this case, the power supply is the volcano which is supposed to supply lava at a constant rate.

The similarity between the three expressions of Eqs. (5) through (7) is obvious, as is the fact that more than one type of power supply can sustain a current. In the case of an electric current (e.g., electrons flowing along a wire), the effect of gravity on the small mass of electrons is irrelevant compared to the effect of the electric potential on the electric charges carried by the same electrons. In this case, gravity is negligible, and the energy involved reduces to Eq. (5). Instead, in the case of an isoviscous gravity current (e.g., Huppert et al. 1982; Garel et al. 2012), the energy involved in movement is governed by Eq. (6), and even if a given amount of heat is released during flow of the current, cooling has no effect on the movement of the flow. The situation changes substantially for a current involving a fluid that cools below the liquid-solid transition (e.g., lava flows or the PEG currents of Garel et al. 2014). However, even in the case of a solidifying current, at the onset of the current, the cooling effect is limited, and the initial phase can be approximated by an isoviscous gravity current (Hulme 1974; Dragoni et al. 1986), as confirmed by the analog experiments of Garel et al. (2014). As time passes, and cooling effects become relevant, the differences between an isoviscous liquid and the cooling lava become important, and the system begins to be governed by Eq. (7).

In both electric currents and lava flows, the "insulation conditions" are crucial (Keszthelyi et al. 1995b; Harris and Rowland 2001, 2009; Harris et al. 2005; 2007b; 2010). In Eq. (5), electric charge is the analog of the liquid lava, and the variation of electric potential is an analog for cooling. While the movement of electric charges (i.e., the electric current) is driven by the balance between electric potential and by

resistance (Ohm's law), the movement of lava is driven by gravity. In the electric circuit shown in Fig. 17a, application of Ohm's law means that  $V = R_1 I_1 = R_2 I_2 = R_3 I_3$ . We can imagine the same potential  $V$  maintained between two opposite poles as in Fig. 17b, and nothing changes in the elements of the circuit. We now take a similar circuit with an arbitrarily large number of elements (e.g., Fig. 17c), still ruled by Ohm's law. The last step is to switch from a steady electric current to a steady lava current (Fig. 17d), where the ALFS has attained balancing mass and energy budgets. In this case, the positive pole is the vent, and negative poles are scattered around the surrounding "lava deposit" systems. At steady state, the mass of the lava parcels exiting the system (per the unit time) balances the input supply and each parcel exiting the ALFS (having mass  $m_p$ ) has completed his own path as ALFS, becoming part of the "lava deposit" having released a heat quantity  $\Delta Q_p$  ( $\Delta Q_p = m_p c_p \Delta T$ , in which  $\Delta T$  is the same as in Eq. 7). In this case, Eq. (7) holds.

Segments of the lava flow system where the rate of heat dissipation is high (e.g., the channelized flows described in Harris et al. 2005 or Lombardo et al. 2009) are analogs for segments of the electric circuit where resistivity is high. Similarly, insulated segments of a lava flow system (e.g., tubes, Keszthelyi 1995b) are analogs to low resistivity segments in the electric circuit. Within the framework of this analogy, it is possible to apply Ohm's to a lava current to obtain a relation between insulation conditions and lava flow length (e.g., Pinkerton and Wilson 1994; Kilburn 2000; Harris & Rowland 2009). If the temperature gap  $\Delta T$  between the eruption temperature and the temperature at which lava parcels exit from the ALFS is assumed to be constant ( $\Delta T$  is analog of  $\Delta V_E$  or  $V$ ), and if a constant intensity in supply  $\Delta m/\Delta t$  is maintained (analog of a given electric current  $I$ ), then the value of the resistance  $R$  can be determined. Considering a constant segment of the conductor constituting a homogeneous circuit (e.g., a wire or channel), then the following relation applies:

$$R \propto \rho L \quad (8)$$

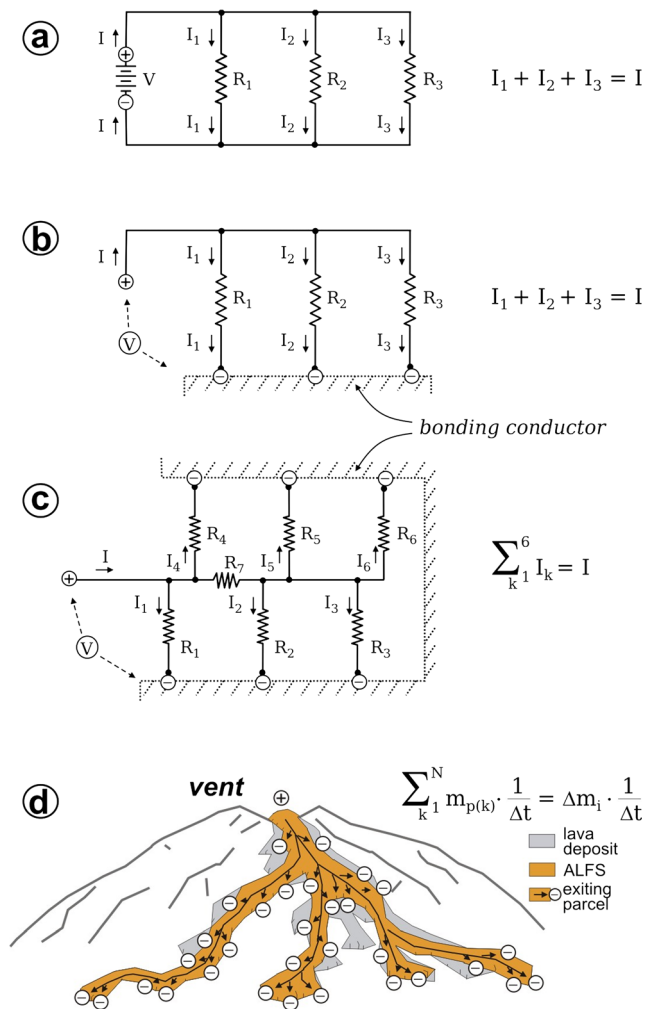


**Fig. 17** From a steady-state electric current in a circuit to a steady-state lava current. **a–c** Electric circuits with increasing complexity. The summation of partial currents over all branches of the circuit is equal to the total current  $I$  flowing out from the positive pole. **d** Sketch of a lava current in steady state, when the summation over all  $N$  lava parcels (each having a mass  $m_p$ ) exiting the ALFS per unit time equals the supply rate from the vent ( $\Delta m_1/\Delta t$ )

where  $\rho$  is the resistivity and  $L$  is the length of the conductor. Relation (8) illustrates that, for a constant  $R$ , an increase in  $\rho$  must be compensated by a proportional decrease in length  $L$  of the circuit. Given the analogy between the insulation conditions in lava flows and the resistivity in electric circuits, insulation determines the length of the lava current at steady state for a given supply rate and  $\Delta T$  through its resistivity effect.

Because steep slopes promote higher fluxes of heat and mass from the ALFS, to balance mass, the ALFS requires formation of a thick, narrow “lava deposit” systems on steep slopes and comparatively thin wide units on shallow slopes (Fig. 18). The overall, counterintuitive implication is that a steeper slope promotes a shorter ALFS length, due to enhanced heat losses and thus accelerated cooling. Two

examples of this cause and effect are given in Fig. 18, where an additional example of low resistivity promoted by shallow slopes is the Carrizozo flow of Keszthelyi and Pieri (1993), where the supply rate was low, slopes shallow but flow length long (~75 km) due to very low rates of heat dissipation. In effect, a tube system was formed to provide extremely effective insulation (Keszthelyi 1995b), so that the final runouts could increase over the case of poorly insulated flow (Harris and Rowland 2009), even though discharge rate is low (Pinkerton and Wilson 1994). The tendency towards flow field thickening on steeper slopes is also promoted by a greater propensity towards flow unit bifurcation (Dietterich and Cashman 2014), which also holds in subaqueous environment (Moore et al. 1971). A bifurcation is intended here as the process of splitting a flow front into two separate units around a morphological obstacle. This process creates two smaller flow units fed by (indicatively) half the supply of the parent flow. According to the Walker’s rule (Walker 1971), this process leads to a shorter runout (Dietterich et al. 2015). However, this process can also be interpreted in terms of an increase in the rate of heat dissipation, because simple geometrical considerations suggest that splitting a flow unit into two smaller units leads to an increase of the cumulative surface area, which promotes a faster heat dissipation (Robertson and Kerr 2010), and thus a shorter expected runout, leading to the formation of a flow field that is highly compound in nature on steep slopes. Behncke et al. (2016), for example, showed how channel-fed flows had a tendency to take on the form of thick, braided compound flow fields on steep slopes during Mt. Etna’s 2008–2009 eruption, a case nearly identical to that of Fig. 18a. Similarly, Gregg and Fink (2000) observed in their analog experiments with PEG extruded at constant rate beneath cold sucrose solution that “contrary to the predicted behaviors of Newtonian and Bingham fluids, pillow mound thickness increases with increasing slope” (Gregg and Fink 2000).

However, there will—of course—be cases where thickening can also be promoted by a sudden decrease in slope (e.g., the Kilauea 2011–2013 lava flow field, Poland 2014) or in basins (e.g., the Etna 1991–1993 flow field, Stevens et al. 1997; or the 1997 Okmok’s caldera lava flow, Patrick et al. 2004) due to accumulation, stagnation, and inflation of units in such locations.

**The least dissipation principle in lava flows**

Ohm’s law (Ohm 1827) was later incorporated into Kirchhoff’s current and voltage laws (Kirchhoff 1848). Although these laws are universally known and widely used in electric circuits, it is much less widely appreciated that they include the first demonstration of the principle of “least dissipation” in steady-state non-equilibrium systems. The least dissipation principle in electric currents states that a current

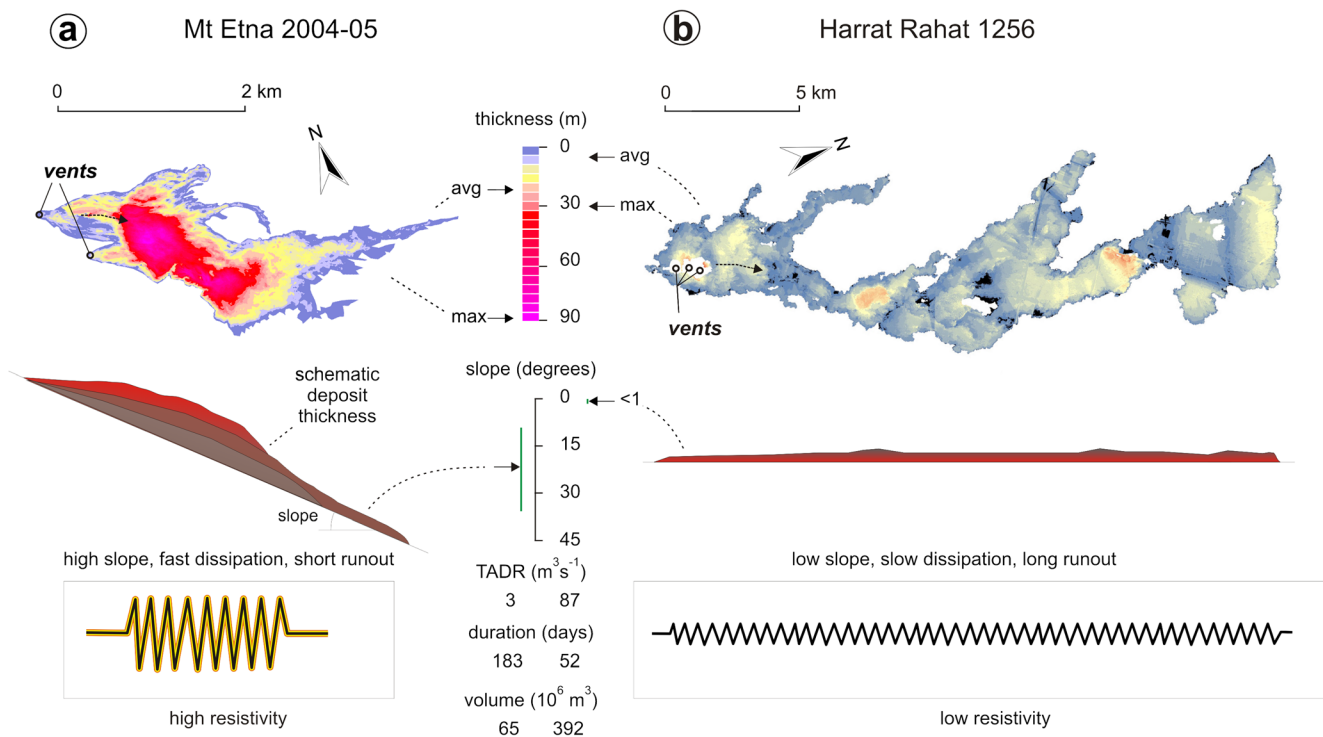


**Fig. 18** Examples of lava flows formed on high and low slopes with related characteristics and analogies with different resistors. The thickness map in **a** is from LIDAR data acquired during multiple acquisitions of Mt. Etna's 2004–2005 lava flow field (Tarquini and Favalli 2010), and that of **b** is modified from Kereszturi et al. (2016).

The two examples differ with respect to several parameters, not only underlying slope but also supply rate, duration, and volume. However, the contrasting final deposits can be considered as indicative as the effects of higher rates of heat dissipation promoted by steeper slopes

distributes itself so as to dissipate as little heat as possible (e.g., Jaynes 1980). Following the early work of Kirchhoff, the same principle of least dissipation showed wide applicability and was extended to other phenomena evolving in stationary non-equilibrium conditions (e.g., acoustics and mechanics; Jaynes 1980). The question now is: can the least dissipation principle also apply to lava flows? A lava current will always be driven by gravity downhill in the steepest direction, this being the path of highest heat dissipation. Hence, if one takes into account only what happens at the propagating front of the flow, it appears that there is no room for the least dissipation principle in lava flows. However, if one considers zones back upflow from the front, more mature portions of flow tend to increase insulation over time. This is true in inflating sheet flows, where the thickening crust decreases heat loss with increasing distance from the flow front (e.g., Harris et al. 2007c; Patrick et al. 2011), and this is also true in channelized flows, where the tendency towards roofing over the open sections with time is ubiquitous (Greeley 1987; Peterson et al. 1994; Calvari and Pinkerton 1998; Bailey et al. 2006; James et al. 2012) and is confirmed by both numerical modeling and analog experiments (Valerio et al. 2008, 2010; Robertson and Kerr 2012a, 2012b). Hence, it appears that a least dissipation principle applies in established portions of flow units, with downhill progression of the front promoting maximum

dissipation locally. Thus, when lava flow units grow in size attaining their maximum extent and forward motion vanishes (i.e., stationary conditions are approached), the system appears to be essentially ruled by the least dissipation principle. We see this effect in the general three-stage trend of flow front advance identified by Kilburn (1996, (1) lengthening, (2) deceleration, and (3) much slower advance) and illustrated in the plots in Fig. 19 where ratio of flow front extension to entire ALFS volumetric expansion decreases with  $1/\text{time}$  for both channelized and sheet flows. This is because the extension of the body of the flow unit grows in extension much more than the front after a period of initial lengthening (Rowland et al. 2005). The average rate of heat dissipation per unit volume of the ALFS thus also decreases with  $1/\text{time}$  accordingly.

### Comparison between lava currents and analog experiments

The expression of the thermal budget introduced here as Eq. (3) includes a transient term which can be compared with the “dynamic” proxy introduced through analog experiments by Garel et al. (2012, 2014, 2015). These experiments explored how a cooling gravity current attains thermal steady state after



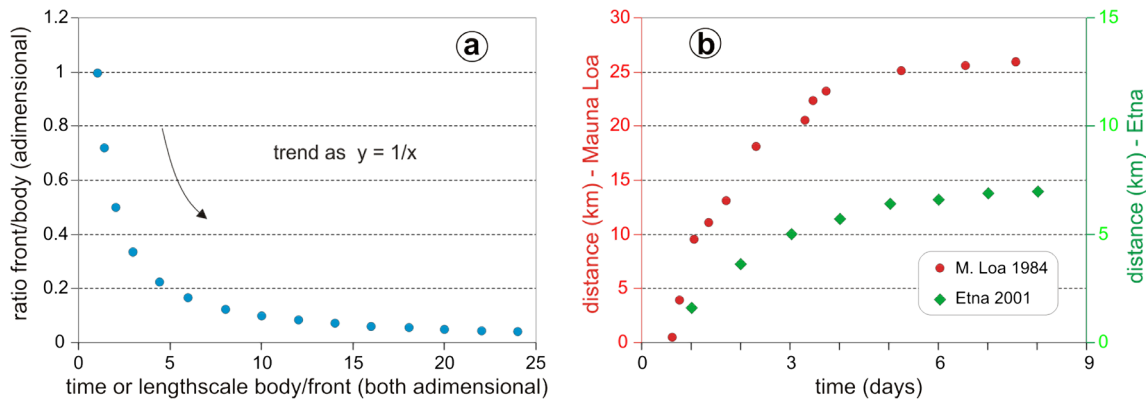


**Fig. 19** Decreasing influence of the flow front as the ALFS lengthens and moves towards steady-state conditions. **a** Ratio of flow front extent to “body” (total ALFS) growth with time. **b** Plots of flow front position vs time for Mauna Loa’s 1984 channel-fed flow (Lipman and Banks 1987) and Mt. Etna’s 2001 LFS1 flow (Behncke and Neri 2003, Coltelli et al.

2007). Notice that, although the supply rate often displays a peaked trend followed by a waning trend (Wadge 1981), during the initial 10 days, the supply of the Mt. Etna’s 2001 LFS1 flow was relatively stable (Coltelli et al. 2007). Plots in **b** have been redrawn from Castruccio et al. (2013)

an initial transient time. In the isoviscous gravity currents of Garel et al. (2012), the advection of heat was only a “passive tracer” that did not affect the movement of the gravity current. If an open system is defined by an arbitrary, fixed boundary placed inside the stationary current, then such a system will always attain a non-equilibrium steady state (NESS) in which both heat and mass budgets are balanced. In the thermal image of Fig. 20a, the flow had already progressed beyond the boundary of the field of view imaged and attained a steady-state condition (see Garel et al. 2012 for details). Owing to the stationary state of the ALFS throughout the field of view, it is possible to trace an arbitrary limit defining a system in which both mass and heat budgets are balanced (e.g., NESS\_a1 and

NESS\_a2, Fig. 18a). Such a system is akin to the system presented in Fig. 3 (i.e., a channel section, in this case for a river). In this case, there is no mass outflow from the system by cooling and solidification, which is the case in an ALFS where mass is transferred to the “lava deposit” system. An isoviscous gravity current is similar to a sheet flow of pahoehoe due to the thickness limit to vertical growth, but striking differences are present, for example an opposite surface thermal profiles are obtained (cf Figs. 4 and 20a) and a static radiating region is obtained by the experiment, as opposed to a dynamic one in a lava sheet flow, where the hotter region moves outwards following the propagating boundary of the flow unit (e.g., Harris et al. 2007c).

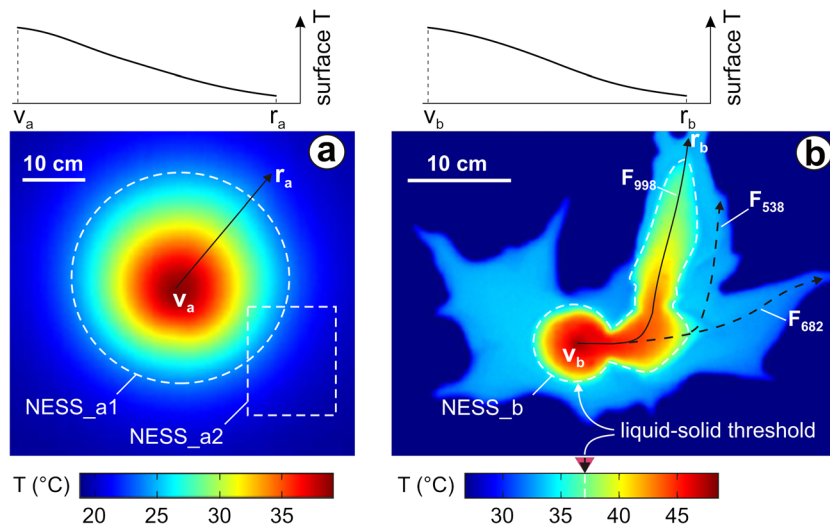


**Fig. 20** Gravity currents from Garel et al. (2012, 2014, 2015). **a** Isoviscous gravity flow in thermal steady state propagating radially from a source ( $v_a$ ). Section  $v_a-r_a$  is used for the relative temperature profile given above (after Garel et al. 2015). **b** Solidifying flow. White dashed line encloses the surface with  $T > 37$  °C (labeled NESS\_b), which

is the solidification temperature of the fluid (PEG). Line  $v_b-r_b$  is used for the relative temperature profile given at top of figure.  $F_{998}$ ,  $F_{682}$ , and  $F_{538}$  indicate the axis of the main active currents at different times:  $t = 998$  s,  $t = 682$  s, and  $t = 538$  s, respectively (after Garel et al. 2015)

In the solidifying currents presented by Garel et al. (2014), the transition from liquid to solid mimics the transition from an ALFS to a “lava deposit” system (Fig. 20b). During the experiments of Garel et al. (2014), the threshold defined by the solidifying temperature of the fluid captures the extent of the liquid system (the ALFS) and indicates attainment of a quasi-steady state after a given transient time (Fig. 12b). This case is akin to a channelized flow, with there being a similar trend in the surface thermal and radiative power profiles between the experiment and natural cases (cf Figs. 4, 12, and 20). An additional similarity is the repeated changes of the main direction of flow advance (Fig. 20b), which is typical of channelized flows (e.g., Guest et al. 1987, Fig. 12e). However, although the end result is the same, there are significant differences between the two processes at work. For example, the transients in the radiative power observed during the emplacement of a channelized flow field (Fig. 12d, e) are due to a diversion process that repeatedly beheads active flow units, which then stagnate and cool, and feed development of new branches. In the case of the experiments, the transients in the radiated power are instead due to sudden overflows to cause a higher amount of hot fluid to be exposed that then undergo rapid cooling (see Garel et al. 2014 for further details). By comparing the two processes, we see that while a diversion halts the increase in radiated power, an overflow triggers an increase. I thus find that, although channelized flows and PEG currents are similar in many respects, a real analog for the process at the heart of the dynamics of channelized flows is not well expressed in the experiments of Garel et al. (2014, 2015). The overflow process is instead more akin to the break-outs iteratively forming at the front of inflating sheet flows, although the surface thermal profiles have opposite trends (cf Figs. 4 and 20).

## Conclusions and perspectives

In reviewing empirical, physical, modeled, and measured relations between mass and energy fluxes at active lava flow units, I have set the state of current knowledge within the basic framework of non-equilibrium thermodynamics. By treating the flowing portion of the system as an open, non-equilibrium system, the physical basis for the thermal approach becomes clearer, and the initial transient time necessary to attain a steady state can be explained in terms of physical, morphological, and dynamic processes. The emerging picture is that a lava flow behaves both (i) as a gravity-driven flow advancing towards the steepest slope and (ii) as a “lava current,” which, through analogy with an electric current, is controlled by the least dissipation principle. Analysis of observations and measurements of actual lava flows highlights that the combined effect of the two principles applies so that gravity (i.e., the topography) is the dominant control during system expansion

and determines the direction of propagation (i.e., the path of the circuit), driving the system towards its maximum extent and maximum rate of mass release. The higher the slope (or the resistivity), the shorter the expected runout (Fig. 18). The least dissipation principle, then, applies to mature portions of flow units, where increasing insulation over time increases the maximum possible runout. Thus, lava moving over flat areas can potentially travel further than lava moving down steep slopes. This apparently counterintuitive conclusion is consistent with documented extremely long (and comparatively thin) lava flows on flat land (e.g., Keszthelyi and Pieri 1993; Stephenson et al. 1998; Solana et al. 2004; Nemeth et al. 2008; Giacomini et al. 2009; Murcia et al. 2014; Bernardi et al. 2015), with the huge extent of flood basalts (e.g., Self et al. 1997; Keszthelyi et al. 2006; Bryan et al. 2010) and with the long runout of Martian lava flows, because lower gravity is functionally equivalent to a lower slope (e.g., Zimbelman 1998; Baloga et al. 2003; Rowland et al. 2004; Garry et al. 2007).

A critical difference between electric currents and lava flows is that the motion of electrons in a wire is almost instantaneous, while lavas build up a “slow-motion” lava circuit over days, weeks, or months along a gravity-driven path. A straightforward consequence of this slow downhill progression is that completion of the “lava circuit” (and hence establishment of steady state) fails if supply is cut before attainment of stationary conditions (Fig. 13). Interestingly, if an effusive eruption lasts long enough, the dynamics of real lava flows promote significant fluctuations in heat dissipation even in the case of constant supply, which is the result of repeated natural diversions (or lava-structural relaxations) which reset the system, which might have otherwise approached steady state, with a balanced heat budget. This evidence highlights a critical aspect of the “dynamic” nature of the thermal signal of lava flows, which is supported by the experimental analysis of Garel et al. (2012, 2014, 2015).

If an effusive eruption lasts long enough under a steady supply rate, a characteristic average duration of flow units tends to emerge, i.e., the structural relaxation time  $\tau_s$ . The limited life span, if other conditions remain constant (e.g., lava characteristics), results in a specific limit of length, and this limit, in the non-equilibrium framework, replaces the concept of cooling-limited length of lava flows.

The duration (or relaxation time  $\tau_s$ ) of lava flow units has received little attention in the literature, probably because this parameter has been expected to be a simple outcome of the cooling-induced limit in length. This explains why a great effort has been produced to constrain the changes in viscosity (e.g., Giordano et al. 2008; Harris and Allen 2008; Costa et al. 2009; Vona et al. 2011; Pistone et al. 2012). Here it is shown that  $\tau_s$  is not simply determined by an increasing viscosity, and that a comprehensive analysis of  $\tau_s$  for different emplacement conditions and different types of flow units is highly desirable

in order to better assess the different factors that determine this crucial parameter, which has a strong impact on the development of long-lasting compound lava flow fields.

The introduction of the ALFS and the consequent analysis of its evolution with time, with continuous mass transfer to the lava deposit system, has substantial implications for lava flow simulations and modeling (e.g., Crisci et al. 2010; Ganci et al. 2012; Bernabeu et al. 2013; Cappello et al. 2015; Cordonnier et al. 2015; Fujita and Nagai 2015; Kelfoun and Vargas, 2016; Tarquini and Favalli 2013, 2015; Mossoux et al. 2016). Lava flow models should account for the possible onset of a structural relaxation time  $\tau_s$  and should account for the mass partition between ALFS and lava deposit system, with consequent modification of the topography. Here I have provided preliminary insights about the partition of the erupted lava between the ALFS and the lava deposit system for the two cases considered, and this new perspective needs to be more widely explored in order to fully exploit the insights that can be gained.

Finally, as long ago suggested by Walker (1973), an additional straightforward implication of lava flow emplacement dynamics is in the interpretation of volcanic landforms (e.g., Karatson et al. 2010; Grosse et al. 2014; Pedersen and Grosse 2014) because the erupted lava is distributed on the existing topography through the iterative formation of flow units. The non-equilibrium perspective introduced here simply provides some additional clues as to how flow units develop.

**Acknowledgements** The author acknowledges the ESF MeMoVoc grant no. 6409. Many thanks go to Diego Coppola for having provided values for the power radiated by the Mt. Etna 2004–2005 eruption and to several colleagues at INGV Pisa for constructive discussions and support (especially F Mazzarini and A Neri). Insightful reviews by Mike James and two anonymous referees, with additional comments from the special editor Andrew Harris, have substantially helped to improve the paper.

## References

- Bailey JE, Harris AJL, Dehn J, Calvari S, Rowland SK (2006) The changing morphology of an open lava channel on Mt. Etna. *Bull Volcanol* 68:497–515
- Barberi F, Brondi F, Carapezza M, Cavarra L, Murgia C (2003) Earthen barriers to control lava flows in the 2001 eruption of Mt. Etna. *J Volcanol Geotherm Res* 123:231–243
- Bartolini S, Becerril L, Martí J (2014) A new Volcanic management Risk Database design (VERDI): application to El Hierro Island (Canary Islands). *J Volcanol Geotherm Res* 288:132–143. doi:10.1016/j.jvolgeores.2014.10.009
- Baloga SM, Glaze LS, Crisp JA, Stockman SA (1998) New statistics for estimating the bulk rheology of active lava flows: Puu Oo examples. *J Geophys Res* 103:5133–5142
- Baloga SM, Mougins-Mark PJ, Glaze LS (2003) Rheology of a long lava flow at Pavonis Mons, Mars. *J Geophys Res* 108(E7):5066. doi:10.1029/2002JE001981
- Behncke B, Neri M (2003) The July–August 2001 eruption of Mt. Etna (Sicily). *Bull Volcanol* 65:461–476
- Behncke B, Fornaciai A, Neri M, Favalli M, Ganci G, Mazzarini F (2016) Lidar surveys reveal eruptive volumes and rates at Etna, 2007–2010. *Geophys Res Lett* 43:4270–4278
- Bernabeu N, Saramito P, Smutek C (2013) Numerical modeling of non-Newtonian viscoplastic flows: part ii. Viscoplastic fluids and general tridimensional topographies. *Int J Numer Anal Model* 11:214–229
- Bernardi MI, Bertotto GW, Jalowitzki TLR, Orihashi Y, Ponce AD (2015) Emplacement history and inflation evidence of a long basaltic lava flow located in Southern Payenia Volcanic Province, Argentina. *J Volcanol Geotherm Res* 293:46–56
- Boekhoven J, Hendriksen WE, Koper GJM, Eelkema R, van Esch JH (2015) Transient assembly of active materials fueled by a chemical reaction. *Science* 349:1075–1079
- Bryan SE, Peate IU, Peate DW, Self S, Jerram DA, Mawby MR, Marsh JSG, Miller JA (2010) The largest volcanic eruptions on Earth. *Earth Sci Rev* 102:207–229
- Burton MR et al (2005) Etna 2004–2005: an archetype for geodynamically-controlled effusive eruptions. *Geophys Res Lett* 32:L09303. doi:10.1029/2005GL022527
- Calvari S, Pinkerton H (1998) Formation of lava tubes and extensive flow field during the 1991–1993 eruption of Mount Etna. *J Geophys Res* 103(B11):27291–27301
- Cappello A, Hérault A, Bilotta G, Ganci G, Del Negro C (2015) MAGFLOW: a physics-based model for the dynamics of lava flow emplacement. In: AJL H, De Groeve T, Garel F, Carn SA (eds) Detecting, modelling and responding to effusive eruptions. Geological Society, London, Special Publications, p 426. doi:10.1144/SP426.16
- Cashman KV, Pinkerton H, Stephenson PJ (1998) Introduction to special section: long lava flows. *J Geophys Res* 103(B11):27281–27289
- Cashman KV, Kerr RC, Griffiths RW (2006) A laboratory model of surface crust formation and disruption on lava flows through non-uniform channels. *Bull Volcanol* 68:753–770
- Cashman KV, Sparks RSJ (2013) How volcanoes work: a 25 year perspective. *Geol Soc Am Bull*. doi:10.1130/B30720.1
- Castruccio A, Rust AC, Sparks RSJ (2013) Evolution of crust- and core-dominated lava flows using scaling analysis. *Bull Volcanol* 75:681. doi:10.1007/s00445-012-0681-2
- Cavagna A (2009) Supercooled liquids for pedestrians. *Phys Rep* 476: 51–124. doi:10.1016/j.physrep.2009.03.003
- Champion D, Le Meste M, Simatos D (2000) Towards an improved understanding of glass transition and relaxations in foods: molecular mobility in the glass transition range. *Trends Food Sci Technol* 11: 41–55
- Chevrel MO, Platz T, Hauber E, Baratoux D, Lavallée Y, Dingwell DB (2013) Lava flow rheology: a comparison of morphological and petrological methods. *Earth Planet Sci Lett* 384:109–120
- Coan T (1844) Journey to Mauna Loa. *Missionary Herald* 40:44–47
- Coltelli M, Proietti C, Branca S, Marsella M, Andronico D, Lodato L (2007) Analysis of the 2001 lava flow eruption of Mt. Etna from three-dimensional mapping. *J Geophys Res* 112(F2)
- Coppola D, Piscopo D, Staudacher T, Cigolini C (2009) Lava discharge rate and effusive pattern at Piton de la Fournaise from MODIS data. *J Volcanol Geotherm Res* 184:174–192
- Coppola D, Laiolo M, Piscopo D, Cigolini C (2013) Rheological control on the radiant density of active lava flows and domes. *J Volcanol Geotherm Res* 249:39–48
- Coppola D, Laiolo M, Cigolini C, Delle Donne D, Ripepe M (2015) Enhanced volcanic hot-spot detection using MODIS IR data: results from the MIROVA system. In: AJL H, De Groeve T, Garel F, Carn SA (eds) Detecting, modelling and responding to effusive eruptions. Geological Society, London, Special Publications, p 426. doi:10.1144/SP426.5
- Cordonnier B, Lev E, Garel F (2015) Benchmarking lava-flow models. In: AJL H, De Groeve T, Garel F, Carn SA (eds) Detecting,

- modelling and responding to effusive eruptions. Geological Society, London, Special Publications, p 426. doi:10.1144/SP426.7
- Costa A, Caricchi L, Bagdassarov N (2009) A model for the rheology of particle-bearing suspensions and partially molten rocks. *Geochem Geophys Geosyst* 10:Q03010. doi:10.1029/2008GC002138
- Crisci GM, Avolio MV, Behncke B, D'Ambrosio D, Di Gregorio S, Lupiano V, Neri M, Rongo R, Spataro W (2010) Predicting the impact of lava flows at Mount Etna, Italy. *J Geophys Res* 115: B04203. doi:10.1029/2009JB006431
- Crisp J, Baloga S (1990) A method for estimating eruption rates of planetary lava flows. *Icarus* 85:512–515
- Danes ZF (1972) Dynamics of lava flows. *J Geophys Res* 77:1430–1432
- Dietterich HR, Cashman KV (2014) Channel networks within lava flows: formation, evolution, and implications for flow behavior. *J Geophys Res*. doi:10.1002/2014JF003103
- Dietterich HR, Cashman KV, Rust AC, Lev E (2015) Diverting lava flows in the lab. *Nat Geosci* 8:494–496
- Dingwell DB (1998) Recent experimental progress in the physical description of silicic magma relevant to explosive volcanism. In: Gilbert JS, RSJ S (eds) *The physics of explosive volcanic eruptions*, vol 145. Geological Society, London, Special Publication, pp 9–26
- Dingwell DB, Webb SL (1989) Structural relaxation in silicate melts and non-newtonian melt rheology in geologic processes. *Phys Chem Miner* 16:508–516
- Dingwell DB, Webb SL (1990) Relaxation in silicate melts. *Eur J Mineral* 2:427–449
- Dozier J (1980) Satellite identification of surface radiant temperature fields of subpixel resolution. NOAA Technical Memorandum, NOAA-81021710. National Earth Satellite Service, Washington DC
- Dragoni M, Bonafede M, Boschi E (1986) Downslope flow models of a Bingham liquid: implications for lava flows. *J Volcanol Geotherm Res* 30:305–325
- Dragoni M, Tallarico A (2009) Assumptions in the evaluation of lava effusion rates from heat radiation. *Geophys Res Lett* 36:L08302. doi:10.1029/2009GL037411
- Duncan AM, Chester DK, Guest JE (1981) Mount Etna volcano: environmental impact and problems of volcanic prediction. *Geogr J* 147: 164–178. doi:10.2307/634532
- Esposti Ongaro T, Cerminara M (2016) Non-equilibrium processes in ash-laden volcanic plumes: new insights from 3D multiphase flow simulations. *J Volcanol Geotherm Res* 326:127–142. doi:10.1016/j.jvolgeores.2016.04.004
- Favalli M, Fornaciari A, Pareschi MT (2009) LIDAR strip adjustment: application to volcanic areas. *Geomorphology* 111:123–135
- Favalli M, Fornaciari A, Mazzarini F, Harris AJL, Neri M, Behncke B, Pareschi MT, Tarquini S, Boschi E (2010) Evolution of an active lava flow field using a multitemporal LIDAR acquisition. *J Geophys Res* 115:B11203. doi:10.1029/2010JB007463
- Favalli M, Tarquini S, Papale P, Fornaciari A, Boschi E (2012b) Lava flow hazard and risk maps at Mount Cameroon volcano. *Bull Volcanol* 74:423–439. doi:10.1007/s00445-011-0540-6
- Favalli M, Tarquini S, Fornaciari A, Boschi E (2012a) Dispersion index of topographic surfaces. *Geomorphology* 153–154:169–178. doi:10.1016/j.geomorph.2012.02.022
- Flynn LP, Mouginiis-Mark PJ (1994) Temperature of an active lava channel from spectral measurements, Kilauea Volcano, Hawaii. *Bull Volcanol* 56:297–301
- Frazzetta G, Romano R (1984) The 1983 Etna eruption: event chronology and morphological evolution of the lava flow. *Bull Volcanol* 47: 1079–1096
- Friedman JD, Williams RS (1968) Infrared sensing of active geologic processes. *Proceedings of the 5th Symposium on Remote Sensing of Environment* 787–820
- Fujita E, Nagai M (2015) LavaSIM: its physical base and applicability. In: AJL H, De Groeve T, Garel F, Carn SA (eds) *Detecting, modelling and responding to effusive eruptions*. Geological Society, London, Special Publications, p 426. doi:10.1144/SP426.14
- Ganci G, Vicari A, Fortuna L, Del Negro C (2011) The HOTSAT volcano monitoring system based on combined use of SEVIRI and MODIS multispectral data. *Ann Geophys* 54:544–550. doi:10.4401/ag-5338
- Ganci G, Vicari A, Cappello A, Negro D (2012) An emergent strategy for volcano hazard assessment: from thermal satellite monitoring to lava flow modeling. *Remote Sens Environ* 119:197–207
- Ganci G, James MR, Calvari S, Del Negro C (2013) Separating the thermal fingerprints of lava flows and simultaneous lava fountaining using ground-based thermal camera and SEVIRI measurements. *Geophys Res Lett* 40:5058–5063. doi:10.1002/grl.50983
- Garel F, Kaminski E, Tait S, Limare A (2012) An experimental study of the surface thermal signature of hot subaerial isoviscous gravity currents: implications for thermal monitoring of lava flows and domes. *J Geophys Res* 117:B02205. doi:10.1029/2011JB008698
- Garel F, Kaminski E, Tait S, Limare A (2014) An analogue study of the influence of solidification on the advance and surface thermal signature of lava flows. *Earth Planet Sci Lett* 396:46–55
- Garel F, Kaminski E, Tait S, Limare A (2015) A fluid dynamics perspective on the interpretation of the surface thermal signal of lava flows. In: AJL H, De Groeve T, Garel F, Carn SA (eds) *Detecting, modelling and responding to effusive eruptions*. Geological Society, London, Special Publications, p 426. doi:10.1144/SP426.6
- Garry WB, Zimbelman JR, Gregg TKP (2007) Morphology and emplacement of a long channeled lava flow near Ascræus Mons Volcano, Mars. *J Geophys Res Planets* 112:E08007. doi:10.1029/2006JE002803
- Giacomini L, Massironi M, Martellato E, Pasquarè G, Frigeri A, Cremonese G (2009) Inflated flows on Daedalia Planum (Mars)? Clues from a comparative analysis with the Payen volcanic complex (Argentina). *Planet Space Sci* 57:556–570. doi:10.1016/j.pss.2008.12.001
- Giordano D, Russel JK, Dingwell DB (2008) Viscosity of magmatic liquids: a model. *Earth Planet Sci Lett* 271:123–134
- Glansdorff P, Prigogine I (1971) *Thermodynamic theory of structure, stability and fluctuations*. Wiley, London ISBN 0-471-30280-5
- Glaze LS, Baloga SM (1998) Dimensions of Pu'u O'o lava flows on Mars. *J Geophys Res* 103:13,659–13,666
- Glaze LS, Baloga SM, Garry WB, Fagents SA, Parcheta C (2009) A hybrid model for leveed lava flows: implications for eruption styles on Mars. *J Geophys Res* 114:E07001. doi:10.1029/2008JE003278
- Goldbeter A (2002) Computational approaches to cellular rhythms. *Nature* 420:238–245
- Greeley R (1987) The role of lava tubes in Hawaiian volcanoes. *US Geol Surv Prof Pap* 1350:1589–1602
- Gregg TKP, Fink JH (2000) A laboratory investigation into the effects of slope on lava flow morphology. *J Volcanol Geotherm Res* 96:145–159
- Gresham D, Hong J (2015) The functional basis of adaptive evolution in chemostats. *FEMS Microbiol Rev* 39:1–19
- Griffiths RW (2000) The dynamics of lava flows. *Annu Rev Fluid Mech* 32:477–518
- Grosse P, Euillades PA, Euillades LD, van Wyk de Vries B (2014) A global database of composite volcano morphometry. *Bull Volcanol* 76:784. doi:10.1007/s00445-013-0784-4
- Gudmundsson MT et al (2016) Gradual caldera collapse at Bárðarbunga volcano, Iceland, regulated by lateral magma outflow. *Science* 353. doi:10.1126/science.aaf8988
- Guest JE, Kilburn CRJ, Pinkerton H, Duncan AM (1987) The evolution of lava flow-fields: observations of the 1981 and 1983 eruptions of Mount Etna, Sicily. *Bull Volcanol* 49:527–540
- Harris AJL (2013) *Thermal remote sensing of active volcanoes: a user's manual*. Cambridge ISBN 978-0-521-85945-5

- Harris AJL, Rowland SK (2001) FLOWGO: a kinematic thermo-rheological model for lava flowing in a channel. *Bull Volcanol* 63: 20–44
- Harris AJL, Ripepe M (2007) Regional earthquake as a trigger for enhanced volcanic activity: evidence from MODIS thermal data. *Geophys Res Lett* 34:L02304. doi:10.1029/2006GL028251
- Harris AJL, Allen JS (2008) One-, two- and three phase viscosity treatments for basaltic lava flows. *J Geophys Res Solid Earth* 113: B09212. doi:10.1029/2007JB005035
- Harris AJL, Baloga SM (2009) Lava discharge rates from satellite-measured heat flux. *Geophys Res Lett* 36:L19302. doi:10.1029/2009GL039717
- Harris AJL, Rowland S (2009) Effusion rate controls on lava flow length and the role of heat loss: a review. In: Thordarson T, Self S, Larsen G, Rowland SK, Hoskuldsson A (eds) *Studies in volcanology: the legacy of George Walker*. In: Special Publications of IAVCEI pp. 33–51
- Harris AJL, Blake S, Rothery DA (1997) A chronology of the 1991 to 1993 Mount Etna eruption using advanced high resolution radiometer data: implications for real-time thermal volcano monitoring. *J Geophys Res* 102(B4):7985–8003
- Harris A, Flynn L, Keszthelyi L, Mougini-Mark P, Rowland S, Resing J (1998) Calculation of lava effusion rates from Landsat TM data. *Bull Volcanol* 60:52–71
- Harris AJL, Bailey J, Calvari S, Dehn J (2005) Heat loss measured at a lava channel and its implications for down-channel cooling and rheology. In: Manga M, Ventura G (eds) *Kinematics and dynamics of lava flows: Geological Society of America Special Paper 396*, p. 125–146. doi: 10.1130/2005.2396(09)
- Harris A, Dehn J, Calvari S (2007a) Lava effusion rate definition and measurement: a review. *Bull Volcanol* 70:1–22
- Harris AJL, Favalli M, Mazzarini F, Pareschi MT (2007c) Best-fit results from application of a thermo-rheological model for channelized lava flow to high spatial resolution morphological data. *Geophys Res Lett* 34:L01301. doi:10.1029/2006GL028126
- Harris AJL, Dehn J, James MR, Hamilton C, Herd R, Lodato L, Steffke A (2007b) Pāhoehoe flow cooling, discharge, and coverage rates from thermal image chronometry. *Geophys Res Lett* 34:L19303
- Harris AJL, Favalli M, Mazzarini F, Hamilton CW (2009) Construction dynamics of a lava channel. *Bull Volcanol* 71:459–474
- Harris AJL, Favalli M, Steffke A, Fornaciari A, Boschi E (2010) A relation between lava discharge rate, thermal insulation, and flow area set using lidar data. *Geophys Res Lett* 37:L20308. doi:10.1029/2010GL044683
- Harris AJL, et al. (2016) Conclusion: recommendations and findings of the RED SEED working group. From: Harris AJL, De Groeve T, Garel F, Carn SA (eds) *Detecting, modelling and responding to effusive eruptions*. Geological Society, London, Special Publications, 426, doi:10.1144/SP426.11
- Harris AJL, Rowland SK, Villeneuve N, Thordarson T (2017) Pāhoehoe, ‘a‘ā, and block lava: an illustrated history of the nomenclature. *Bull Volcanol* 79:7. doi:10.1007/s00445-016-1075-7
- Herdervari P (1963) On the energy and magnitude of volcanic eruptions. *Bull Volcanol* 25:373–385
- Hoblitt RP, Orr TR, Heliker C, Denlinger RP, Hon K, Cervelli PF (2012) Inflation rates, rifts, and bands in a pāhoehoe sheet flow. *Geosphere* 8(5):179–195. doi:10.1130/GES00656.1
- Hon K, Kauahikaua J, Denlinger R, Mackay K (1994) Emplacement and inflation of pāhoehoe sheet flows: observations and measurements of active lava flows on Kilauea Volcano, Hawaii. *Geol Soc Am Bull* 3:351–370
- Hulme G (1974) The interpretation of lava flow morphology. *Geophys J R Astron Soc* 39:361–383
- Huppert H, Shepherd J, Sigurdsson H, Sparks R (1982) On lava dome growth, with application to the 1979 lava extrusion of the Soufriere of St. Vincent. *J Volcanol Geotherm Res* 14:199–222
- James MR, Bagdassarov N, Muller K, Pinkerton H (2004) Viscoelastic behavior of basaltic lavas. *J Volcanol Geotherm Res* 132:99–113
- James MR, Robson S, Pinkerton H, Ball M (2006) Oblique photogrammetry with visible and thermal images of active lava flows. *Bull Volcanol* 69:105–108. doi:10.1007/s00445-006-0062-9
- James MR, Pinkerton H, Robson S (2007) Image based measurement of flux variation in distal regions of active lava flows. *Geochem Geophys Geosyst* 8:Q03006. doi:10.1029/2006GC001448
- James MR, Pinkerton H, Applegarth LJ (2009) Detecting the development of active lava flow fields with a very-long-range terrestrial laser scanner and thermal imagery. *Geophys Res Lett* 36:L22305. doi:10.1029/2009GL040701
- James MR, Applegarth LJ, Pinkerton H (2012) Lava channel roofing, overflows, breaches and switching: insights from the 2008–2009 eruption of Mt. Etna. *Bull Volcanol* 74:107–117
- Jaynes ET (1980) The minimum entropy production principle. *Annu Rev Phys Chem* 31:579–601
- Jones JG (1968) Pillow lava and pāhoehoe. *J Geol* 76:485–488
- Karátson D, Favalli M, Tarquini S, Fornaciari A, Wörner G (2010) The regular shape of stratovolcanoes: a DEM-based morphometrical approach. *J Volcanol Geotherm Res* 193:171–181. doi:10.1016/j.jvolgeores.2010.03.012
- Kauahikaua J, Cashman KV, Mattox TN, Heliker CC, Hon KA, Mangan MT, Thornber CR (1998) Observations on basaltic lava streams in tubes from Kilauea Volcano, island of Hawai‘i. *J Geophys Res* 103(B11):27.303–27.323
- Kelfoun K, Vargas SV (2016) VolcFlow capabilities and potential development for the simulation of lava flows. From: Harris AJL, De Groeve T, Garel F, Carn SA (eds) *Detecting, modelling and responding to effusive eruptions*. Geological Society, London, Special Publications, 426, doi:10.1144/SP426.8
- Kereszturi G, Németh K, Moufti MR, Cappello A, Murcia H, Ganci G, Del Negro C, Procter J, Zahran HMA (2016) Emplacement conditions of the 1256AD Al-Madinah lava flow field in Harrat Rahat, Kingdom of Saudi Arabia—insights from surface morphology and lava flow simulations. *J Volcanol Geotherm Res* 309:14–30
- Kerr RC, Griffiths RW, Cashman KV (2006) Formation of channelized lava flows on an unconfined slope. *J Geophys Res* 111:B10206. doi: 10.1029/2005JB004225
- Keszthelyi L (1995a) Measurements of cooling at the base of pāhoehoe flows. *Geophys Res Lett* 22:2195–2198
- Keszthelyi L (1995b) A preliminary thermal budget for lava tubes on Earth and planets. *J Geophys Res* 100:20,411–20,420
- Keszthelyi LP, Pieri DC (1993) Emplacement of the 75-kmlong Carrizozo lava flow field, south-central New Mexico. *J Volcanol Geotherm Res* 59:59–75
- Keszthelyi L, Denlinger R (1996) The initial cooling of pāhoehoe flow lobes. *Bull Volcanol* 58:5–18
- Keszthelyi L, Thordarson T, McEwen A, Haack H, Guilbaud M-N, Self S, Rossi MJ (2004) Icelandic analogs to Martian flood lavas. *Geochem Geophys Geosyst* 5:Q11014. doi:10.1029/2004GC000758
- Keszthelyi L, Self S, Thordarson T (2006) Flood lavas on Earth, Io and Mars. *J Geol Soc* 163(2):253–264
- Kilburn CRJ (1996) Patterns and predictability in the emplacement of subaerial lava flows and flow fields. In: Scarpa R, Tilling RI (eds) *Monitoring and mitigation of volcano hazards*. Springer, Berlin, pp 491–537. doi:10.1007/978-3-642-80087-0\_15
- Kilburn CRJ (2000) Lava flows and flow fields. In: Sigurdsson H (ed) *Encyclopedia of volcanoes*. Academic Press, San Diego, CA, pp 291–306
- Kilburn CRJ, Lopes R (1988) The growth of aa lava flow fields on Mount Etna, Sicily. *J Geophys Res Solid Earth* 93:14759–14772
- Kilburn CRJ, Lopes R (1991) General patterns of flow field growth: Aa and blocky lavas. *J Geophys Res Solid Earth* 96:19721–19732

- Kirchhoff GD (1848) Ueber die anwendbarkeit der formeln für die intensitäten der galvanischen strome in einem systeme leucarer leiter auf systeme, die zum theil nicht aus linearen leitern bestehen. *Ann Phys* 75:189–205
- Kleidon A. (2010) Non-equilibrium thermodynamics, maximum entropy production and Earth-system evolution. *Philosophical Transactions of the Royal Society of London A: Mathematical, Physical and Engineering Sciences*
- Kolzenburg S, Giordano D, Cimarelli C, Dingwell DB (2016) In situ thermal characterization of cooling/crystallizing lavas during rheology measurements and implications for lava flow emplacement. *Geochim Cosmochim Acta* 195:244–258
- Kolzenburg S, Giordano D, Thordarson T, Höskuldsson A, Dingwell DB (2017) The rheological evolution of the 2014/2015 eruption at Holuhraun, central Iceland. *Bull Volcanol* 79:45. doi:10.1007/s00445-017-1128-6
- La Spina G, Burton M, de' Michieli Vitturi M, Arzilli F (2016) Role of syn-eruptive plagioclase disequilibrium crystallization in basaltic magma ascent dynamics. *Nat Commun* 7:13402. doi:10.1038/ncomms13402
- Larini L, Ottochian A, De Michele C, Leporini D (2008) Universal scaling between structural relaxation and vibrational dynamics in glass-forming liquids and polymers. *Nat Phys* 4:42–45
- Lipman PW, Banks NG (1987) Aa flow dynamics, Mauna Loa. In: Decker W, Wright TL, Stauffer PH (eds) *Volcanism in Hawaii*. US Geol Surv prof paper no. 1350, pp 1527–1567
- Lockwood JP, Hazlett RW (2010) *Volcanoes global perspectives*. Wiley-Blackwell
- Lombardo V, Harris AJL, Calvari S, Buongiorno MF (2009) Spatial variations in lava flow field thermal structure and effusion rate derived from high spatial resolution hyperspectral (MIVIS) data. *J Geophys Res* 114:B02208. doi:10.1029/2008JB005648
- Lombardo V (2016) Influence of pre-existing topography on downflow lava discharge rates estimated from thermal infrared airborne data. *Geophys J Int* 205:122–133. doi:10.1093/gji/ggv557
- Malin MC (1980) Lengths of Hawaiian lava flows. *Geology* 8:306–308
- Mastin LG, Ghiorso MS (2001) Adiabatic temperature changes of magma-gas mixtures during ascent and eruption. *Contrib Mineral Petrol* 141:307–321
- Mattox TN, Heliker C, Kauahikaua J, Hon K (1993) Development of the 1990 Kalapana flow field, Kilauea Volcano, Hawaii. *Bull Volcanol* 55:407–413. doi:10.1007/BF00302000
- Mazzarini F, Pareschi MT, Favalli M, Isola I, Tarquini S, Boschi E (2005) Morphology of basaltic lava channels during the Mt. Etna September 2004 eruption from airborne laser altimeter data. *Geophys Res Lett* 32:L04305
- McCabe MF, Balick LK, Theiler J, Gillespie AR, Mushkin A (2008) Linear mixing in thermal infrared temperature retrieval. *Int J Remote Sens* 29:5047–5061
- Miyamoto H, Papp KR (2004) Rheology and topography control the path of a lava flow: insight from numerical simulations over a preexisting topography. *Geophys Res Lett* 31:L166085. doi:10.1029/2004GL020626
- Moore JG (1975) Mechanism of formation of pillow lava. *Am Sci* 63: 269–277
- Moore JG, Cristofolini R, Lo Giudice A (1971) Development of pillows on the submarine extension of recent lava flows, Mount Etna, Sicily US Geol Surv Prof Paper no 750-C, pp C89–C97
- Moore HJ (1987) Preliminary estimates of the rheological properties of 1984 Mauna Loa lava. In: Decker RW et al. (ed) *Volcanism in Hawaii*, in US Geol Surv Prof Pap 1350:1569–1588
- Mossoux S, Saey M, Bartolini S, Poppe S, Canters F, Kervyn M (2016) Q-LAVHA: a flexible GIS plugin to simulate lava flows. *Comput Geosci* 97:98–109. doi:10.1016/j.cageo.2016.09.003
- Murcia H, Németh K, Moufti MR, Lindsay JM, El-Masry N, Cronin SJ, Qaddah A, Smith IEM (2014) Late Holocene lava flow morphotypes of northern Hattat Rahat, Kingdom of Saudi Arabia: implications for the description of continental lava fields. *J Asian Earth Sci* 84:131–145. doi:10.1016/j.jseas.2013.10.002
- Németh K, Haller MJ, Martin U, Risso C, Massafiero G (2008) Morphology of lava tumuli from Mendoza (Argentina), Patagonia (Argentina), and Al-Haruj (Libya). *Z Geomorphol* 52:181–194. doi:10.1127/0372-8854/2008/0052-0181
- Nichols RL (1936) Flow-units in basalt. *J Geol* 44:617–630
- Ohm GS (1827) *Die Galvanische Kette*, Mathematisch Bearbeitet 250. **Kessinger**
- Oppenheimer C (1993) Thermal distributions of hot volcanic surfaces constrained using three infrared bands of remote sensing data. *Geophys Res Lett* 20:431–434
- Ottochian A, De Michele C, Puosi F, Leporini D (2012) Disordered systems: predicting the ultra-slow processes by picosecond dynamics. *Il Nuovo Saggiatore* 28:5–10
- Patrick M, Dehn J, Dean K (2004) Numerical modeling of lava flow cooling applied to the 1997 Okmok eruption: approach and analysis. *J Geophys Res* 109:B03202. doi:10.1029/2003JB002537
- Patrick MR, Orr T, Wilson D, Dow D, Freeman R (2011) Cyclic spattering, seismic tremor, and surface fluctuation within a perched lava channel, Kilauea Volcano. *Bulletin of volcanology* 73:639–653.
- Park S, Iversen JD (1984) Dynamics of lava flow: thickness growth characteristics of steady two-dimensional flow. *Geophys Res Lett* 11:641–644
- Pedersen GBM, Grosse P (2014) Morphometry of subaerial shield volcanoes and glaciovolcanoes from Reykjanes Peninsula, Iceland: effects of eruption environment. *J Volcanol Geotherm Res* 282:115–133
- Pedersen GBM et al, the IES eruption team (2017) Lava field evolution and emplacement dynamics of the 2014–2015 basaltic fissure eruption at Holuhraun, Iceland. *J Volcanol Geotherm Res*. doi:10.1016/j.jvolgeores.2017.02.027
- Peterson DW, Holcomb RT, Tilling RI, Christiansen RL (1994) Development of lava tubes in the light of observations at Mauna Ulu, Kilauea Volcano, Hawaii. *Bull Volcanol* 56:343–360
- Pieri DC, Baloga SM (1986) Eruption rate, area, and length relationships for some Hawaiian lava flows. *J Volcanol Geotherm Res* 30:29–45
- Pinkerton H, Wilson L (1994) Factors controlling the lengths of channelled lava flows. *Bull Volcanol* 56:108–120
- Pistone M, Caricchi L et al (2012) Deformation experiments of bubble- and crystal-bearing magmas: rheological and microstructural analysis. *J Geophys Res* 117:B05208. doi:10.1029/2011JB008986
- Poland MP (2014) Time-averaged discharge rate of subaerial lava at Kilauea Volcano, Hawaii, measured from TanDEM-X interferometry: implications for magma supply and storage during 2011–2013. *J Geophys Res* 119:5464–5481. doi:10.1002/2014JB011132
- Ramsey MS, Harris AJL (2012) Volcanology 2020: how will thermal remote sensing of volcanic surface activity evolve over the next decade? *J Volcanol Geotherm Res* 249:217–233
- Richter N, Favalli M, de Zeeuw-van Dalssen E, Fornaciai A, da Silva Fernandes RN, Perez Rodriguez N, Levy J, Silva Victória S, Walter TR (2016) Lava flow hazard at Fogo Volcano, Cape Verde, before and after the 2014–2015 eruption. *Nat Hazards Earth Syst Sci Discuss*. doi:10.5194/nhess-2016-81
- Robertson JC, Kerr RC (2010) Rheological controls on the dynamics of channelled lava flows. 17th Australasian Fluid Mechanics Conference Auckland, New Zealand 5–9 December 2010
- Robertson JC, Kerr RC (2012a) Isothermal dynamics of channelled viscoplastic lava flows and new methods for estimating lava rheology. *J Geophys Res* 117:B01202. doi:10.1029/2011JB008550
- Robertson JC, Kerr RC (2012b) Solidification dynamics in channelled viscoplastic lava flows. *J Geophys Res* 117:B07206. doi:10.1029/2012JB009163

- Rothery DA, Francis PW, Wood CA (1988) Volcano monitoring using short wavelength infrared data from satellites. *J Geophys Res* 93: 7993–8008
- Rowland SK, Harris AJL, Garbeil H (2004) Effects of Martian conditions on numerically modeled, cooling-limited, channelized lava flows. *J Geophys Res* 109:E10010. doi:10.1029/2004JE002288
- Rowland SK, Garbeil H, Harris AJL (2005) Lengths and hazards from channel-fed lava flows on Mauna Loa, Hawai'i, determined from thermal and downslope modeling with FLOWGO. *Bull Volcanol* 67:634–647. doi:10.1007/s00445-004-0399-x
- Scandone R, (1979) Effusion rate and energy balance of Paricutin eruption (1943–1952), Michoacan, Mexico. *Journal of Volcanology and Geothermal Research* 6:49–59
- Self S, Thordarson T, Keszthelyi L, Walker GPL, Hon K, Murphy MT, Long P, Finnemore S (1996) A new model for the emplacement of Columbia River basalts as large, inflated pahoehoe lava flow fields. *Geophys Res Lett* 23:2689–2692
- Self S, Thordarson T, Keszthelyi L (1997) Emplacement of continental flood basalt lava flows. *Large Igneous Provinces: continental, oceanic, and planetary flood volcanism*, 381–410
- Self S, Keszthelyi L, Thordarson T (1998) The importance of pahoehoe. *Annu Rev Earth Planet Sci* 26:81–110
- Solana MC, Kilburn CRJ, Rodriguez Badiola E, Aparicio A (2004) Fast emplacement of extensive pahoehoe flow-fields: the case of the 1736 flows from Montana de las Nueces, Lanzarote. *J Volcanol Geotherm Res* 132:189–207
- Sparks RSJ, Pinkerton H, Hulme G (1976) Classification and formation of lava levee on Mount Etna Sicily. *Geology* 4:269–271
- Stephenson PJ, Burch-Johnston AT, Stanton D, Whitehead PW (1998) Three long lava flows in north Queensland. *J Geophys Res* 103:27, 359–27,370
- Stevens NF, Murray JB, Wadge G (1997) The volume and shape of the 1991–1993 lava flow field at Mount Etna, Sicily. *Bull Volcanol* 58: 449–454
- Tarquini S, de' Michieli Vitturi M (2014) Influence of fluctuating supply on the emplacement dynamics of channelized lava flows. *Bull Volcanol* 76:801. doi:10.1007/s00445-014-0801-2
- Tarquini S, Favalli M (2010) Changes of the susceptibility to lava flow invasion induced by morphological modifications of an active volcano: the case of Mount Etna, Italy. *Nat Hazards* 54:537–546
- Tarquini S, Favalli M (2011) Mapping and DOWNFLOW simulation of recent lava flow fields at Mount Etna. *J Volcanol Geotherm Res* 204: 27–39. doi:10.1016/j.jvolgeores.2011.05.001
- Tarquini S, Favalli M (2013) Uncertainties in lava flow hazard maps derived from numerical simulations: the case study of Mount Etna. *J Volcanol Geotherm Res* 260:90–102. doi:10.1016/j.jvolgeores.2013.04.01
- Tarquini S, Favalli M (2015) Simulating the area covered by lava flows using the DOWNFLOW code. In: AJL H, De Groeve T, Garel F, Carn SA (eds) *Detecting, modelling and responding to effusive eruptions*. Geological Society, London, Special Publications, p 426. doi:10.1144/SP426.15
- Tarquini S, Favalli M, Mazzarini F, Isola I, Fornaciai A (2012a) Morphometric analysis of lava flow units: case study over LIDAR-derived topography at Mount Etna, Italy. *J Volcanol Geotherm Res* 235–236:11–22
- Tarquini S, Vinci S, Favalli M, Doumaz F, Fornaciai A, Nannipieri L (2012b) Release of a 10-m-resolution DEM for the Italian territory: comparison with global-coverage DEMs and anaglyph-mode exploration via the web. *Comput Geosci* 38:168–170. doi:10.1016/j.cageo.2011.04.018
- Thordarson T, Self S (1998) The Roza Member, Columbia River Basalt Group: a gigantic pahoehoe lava flow field formed by endogenous processes? *J Geophys Res* 103(B11):27,411–27,445
- Valerio A, Tallarico A, Dragoni M (2008) Mechanisms of formation of lava tubes. *J Geophys Res* 113:B08209. doi:10.1029/2007JB005435
- Valerio A, Tallarico A, Dragoni M (2010) A model for the formation of lava tubes by the growth of the crust from the levees. *J Geophys Res* 115:B09208. doi:10.1029/2009JB006598
- Vicari A, Cirauddo A, Del Negro C, Herault A, Fortuna L (2009) Lava flow simulations using discharge rates from thermal infrared satellite imagery during the 2006 Etna eruption. *Nat Hazards* 50:539–550
- Vona A, Romano C, Dingwell DB, Giordano D (2011) The rheology of crystal-bearing basaltic magmas from Stromboli and Etna. *Geochim Cosmochim Acta* 75:3214–3236. doi:10.1016/j.gca.2011.03.031
- Vye-Brown C, Self S, Barry TL (2013) Architecture and emplacement of flood basalt flow fields: case studies from the Columbia River Basalt Group, NW USA. *Bull Volcanol* 75:697. doi:10.1007/s00445-013-0697-2
- Wadge G (1978) Effusion rate and the shape of aa lava flow-fields on Mount Etna. *Geology* 6:503–506
- Wadge G (1981) The variation of magma discharge during basaltic eruptions. *J Volcanol Geotherm Res* 2-4:139–168
- Wadge G, Cole P, Stinton A, Komorowski J-C, Stewart R, Toombs AC (2011) Rapid topographic change measured by high resolution satellite radar at Soufriere Hills Volcano, Montserrat 2008–2010. *J Volcanol Geotherm Res* 199:142–152. doi:10.1016/j.jvolgeores.2010.10.011
- Wadge G, Saunders S, Itikarai I (2012) Pulsatory andesite lava flow at Bagana Volcano. *Geochem Geophys Geosyst* 13:Q11011. doi:10.1029/2012GC004336
- Walgraef D (1996) Spatio-temporal pattern formation with examples from physics, chemistry, and material science. Springer, New York
- Walker GPL (1971) Compound and simple lava flows and flood basalts. *Bull Volcanol* 35:579–590
- Walker GPL (1973) Lengths of lava flows. *Philos Trans R Soc Lond A Math Phys Eng Sci* 274:107–118
- Walker GPL (1992) Morphometric study of pillow-size spectrum among pillow lavas. *Bull Volcanol* 54:459–474
- Wilson L, Pinkerton H, Head JW, Roberts KM (1993) A classification scheme for the morphology of lava flow fields. *Lunar Planet Sci XXXIV*:123–124
- Wooster M, Wright R, Blake S, Rothery D (1997) Cooling mechanisms and an approximate thermal budget for the 1991–1993 Mount Etna lava flow. *Geophys Res Lett* 24:3277–3280
- Wright R, Blake S, Harris AJL, Rothery DA (2001) A simple explanation for the space-based calculation of lava eruption rates. *Earth Planet Sci Lett* 192:223–233
- Wright R, Garbeil H, Davies AG (2010) Cooling rate of some active lavas determined using an orbital imaging spectrometer. *J Geophys Res* 115:B06205. doi:10.1029/2009JB006536
- Yokoyama I (1957) Energetics in active volcanoes. 2nd paper. *Bull Earthquake Res Inst* 35:75–97
- Zimbelman JR (1998) Emplacement of long lava flows on planetary surfaces. *J Geophys Res* 103(B11):27,503–27,516